Identification, characterization of Apyrase (*APY*) gene family in rice (*Oryza sativa*) and analysis of the expression pattern under various stress conditions

Aniqua Tasnim Chowdhury[1], Md. Nazmul Hasan[1], Fahmid H Bhuiyan[2], Md. Qamrul Islam[1], Md. Rakib Wazed Nayon[1], Md. Mashiur Rahaman[1,3], Hammadul Hoque[1], Nurnabi Azad Jewel[1], Md Ashrafuzzaman[1], Shamsul H. Prodhan[1*]

[1]Department of Genetic Engineering and Biotechnology, School of Life Sciences, Shahjalal University of Science and Technology, Sylhet, Bangladesh

[2]Plant Biotechnology Division, National Institute of Biotechnology, Ganakbari, Ashulia, Savar, Dhaka, Bangladesh

[3]Institute of Epidemiology, Disease Control and Research (IEDCR), Dhaka, Bangladesh

*Corresponding Author

E-mail: shamsulhp-btc@sust.edu (SHP)

Abstract

Apyrase (*APY*) is a nucleoside triphosphate (NTP) diphosphohydrolase (NTPDase) which is a member of the superfamily of guanosine diphosphatase 1 (GDA1) - cluster of differentiation 39 (CD39) nucleoside phosphatase. Under various circumstances like stress, cell growth, the extracellular adenosine triphosphate (eATP) level increases, causing a detrimental influence on cells such as cell growth retardation, ROS production, NO burst, and apoptosis. Apyrase hydrolyses eATP accumulated in the extracellular membrane during stress, wounds, into adenosine diphosphate (ADP) and adenosine monophosphate (AMP) and regulates the stress-responsive pathway in plants. This study was designed for the identification, characterization, and for analysis of *APY* gene expression in *Oryza sativa*. This investigation discovered nine *APY*s in rice, including both endo- and ecto-apyrase. According to duplication event analysis, in the evolution of *OsAPY*s, a significant role is performed by segmental duplication. Their role in stress control, hormonal responsiveness, and the development of cells is supported by the corresponding cis-elements present in their promoter regions. According to expression profiling by RNA-seq data, the genes were expressed in various tissues. Upon exposure to a variety of biotic as well as abiotic stimuli, including anoxia, drought, submergence, alkali, heat, dehydration, salt, and cold, they showed a differential expression pattern. The expression analysis from the RT-qPCR data also showed expression under various abiotic stress conditions, comprising cold, salinity, cadmium, drought, submergence, and especially heat stress. This finding will pave the way for future *in-vivo* analysis, unveil the molecular mechanisms of *APY* genes in stress response, and contribute to the development of stress-tolerant rice varieties.

Keywords: Rice, Apyrase, Abiotic and biotic stress, Conserved motif, Protein structure, Cis-regulatory elements, Expression pattern.

Introduction

Apyrase (*APY*), which is a class of nucleoside triphosphate (NTP) diphosphohydrolase (NTPDase) and a member of the superfamily of GDA1-CD39 (guanosine diphosphatase 1-cluster of differentiation 39) nucleoside phosphatase [1], mediates the concentrations of NTP (nucleoside triphosphate) and NDP (nucleoside diphosphate) [2], especially of ATP (adenosine triphosphate) and ADP (adenosine diphosphate) and catalyzes their breakdown and converts them into ADP and AMP (adenosine monophosphate) [3,4]. ATP, the pervasive intracellular energy resource in every cell, functions in a stress-dependent fashion as it promotes cell growth and development when present in lower concentrations. When the plant cells encounter wound [5], pathogen elicitors ([6,7], cell growth [8], abiotic stress ([9,10], touch [9,11], they discharge ATP into the extracellular matrix (ECM) where it becomes known as eATP (extracellular ATP). Usually, these stresses befall simultaneously and include cross-talk from numerous hormones and signaling pathways [12,13]. Survival of plants [8], development [4,6,14] gravitropism [15], plant defense strategy [16], cellular apoptosis [17], stress responsiveness [3,5,9,18], are controlled by eATP. Under such circumstances, the eATP level rises, giving rise to many negative impacts on cells like inhibiting the rate of cell growth [19], ROS (reactive oxygen species) production, NO (nitric oxide) burst, as well as triggering apoptosis [20]. At this point, *APY* comes into action by breaking down eATP, which helps plants in cell survival, growth, development, and face off several stresses [21].

The characteristic feature of NTPDase family proteins is to contain five apyrase conserved regions (ACRs) [22], and APYs can be separated as ecto-and endo-APY, as per the subcellular localization [23]. Ecto-APYs are situated on the cell's surface, and the ones located on cytoplasmic organelles are generally called endo-apyrases. Many apyrase genes include transmembrane domains at their N- and C- terminals [24] and generally feature amino acid

glycosylation, which is necessary to ensure proper folding of proteins, targeting at the membrane, cellular distribution, and enzymatic function [1]. However, APYs are not similar to ATPases such as APYs can employ several divalent cofactors like Mn^{2+}, Zn^{2+}, Ca^{2+}, and Mg^{2+}, in contrast to ATPases, which employ Mg^{2+} as a cofactor [25]. It also demonstrates insensitivity towards alkaline phosphatase as well as to certain types of ATPase inhibitors [26].

There are several plant species in which *APY*s were discovered, including potato [27,28], *Arabidopsis* [2], soybean [29], cotton [30], wheat [23]. Especially in *Arabidopsis* and wheat, the gene family has been intensively studied. 7 *APY* members in *Arabidopsis* have been identified and described [2]. AtAPY1 and AtAPY2 are endo-APYs as they are found in the Golgi body. They control various cellular phases [2,31], and their mutation can dramatically increase extracellular ATP (eATP), which confirms that APYs located intracellularly might also be able to control eATP homeostasis [4,19]. Others are ecto-APYs, and there have been many pieces of evidence about the involvement of ecto-APYs in the hydrolyzing of eATP [17]. Two other AtAPYs, AtAPY6 and AtAPY7, are also essential to pollen production by controlling the synthesis of polysaccharides [32]. Nine *APY* members were identified in wheat with different expression patterns when subjected to various stresses and even in different tissues [23]. In many species, *APY*s have been found to have involvement in different stress tolerance, such as tolerance towards salinity and drought conditions in *Arabidopsis* after overexpression of *PeAPY1* and *PeAPY2* [33], tolerance to waterlogging in soybean [34]. *PsAPY*, when expressed ectopically, has been reported to exhibit resistance in tobacco to pathogen attack [35]. However, the total signaling pathway working behind the activity of *APY* is still not explained.

Rice is among the world's most widely grown as well as consumed cereals. The majority of the world relies on rice as a main meal [36]. Agricultural production is at risk due to climate change. Likewise, rice production is being hampered due to climate anomalies, including

93 submergence, less rainfall, cold weather, increasing salinity levels, and many more. Fungal and
94 bacterial blight are two of the most severe and prevalent rice diseases that reduce annual rice
95 production [37]. Promoting stress-resistant rice may increase productivity tremendously as the
96 genome-editing and genetic transfer technologies are improving rapidly; these techniques have
97 created an opportunity to produce stress-resistant crops. With the availability of information
98 on the genomes for several crop species during recent years, a systematic genome-wide study
99 has been readily accessible on stress-associated gene families utilizing bioinformatics
100 techniques. Rice is the first food grain of which the entire genome sequence is available [37].
101 It provides a chance to locate the genes and systematically categorize the genes and
102 biochemical pathways essential for expanding rice production, conferring tolerance towards
103 several stresses, as well as enhancing the product's quality.

104 Different families of genes such as *PYL* [38], *NAC* [39], *GRAS* [40], *MYB* [41], *WRKY* [42],
105 *DREB* [43] were reported in rice as gene families associated with responsiveness towards
106 stress. Many genes have been reported to show specific responses when subjected to different
107 stress conditions. For example, cold, high salinity, and drought are associated with the
108 induction of *OsNAC6/SNAC2* [44]. During dehydration, the HKT-1 protein is required for cell
109 osmoregulation and the maintenance of turgor [45]; the HSP20 family provides tolerance to
110 prolonged heat stress and resistance to different environmental stresses [44]. The CRT/DREBP
111 protein family is mainly regulated by cold stress; on the other hand, DREBP (DRE-binding
112 protein) family induction is caused by drought and high salt stress [46]. Overexpression of
113 different genes responsive to stress in rice could increase the tolerance level when subjected to
114 such stress. Such genes include *OsNHX1* in salt stress [47], *OsDREB* under drought conditions
115 [48], *Sub1A* when subjected to submergence stress [49]. Identifying and characterizing such
116 genes responsive to stresses and applying molecular methods could pave the way toward
117 developing rice varieties tolerant of several stresses.

Since there is ample evidence about the role of *APY*s during the stress response, their identifying and characterizing in plants might help find new development sites for strengthening responsiveness towards several stresses through different gene modification methods. There is an absence of studies about *APY*s in rice. The purpose of this research was to characterize *APY* genes in *O. sativa* and provide insight into their function throughout development and in response to stress by doing a genome-wide identification and analyzing their expression profiles. Rice *APY* family members were identified using bioinformatics techniques throughout this study. We further studied the functional characterization, including phylogenetic relationship analysis with the *APY*s from *Arabidopsis* and wheat. Both RT-qPCR and RNA-seq data were utilized in profiling the pattern of gene expression of the *OsAPY*s and suggested their importance in the process of development as well as response to stress. Conclusively, this result will provide a foothold in further analyzing the roles of *OsAPY* in different stress conditions and in identifying targets to enhance rice's tolerance level under various stresses.

Materials and methods

Identification of *APY* family members in *Oryza sativa*

The TAIR database (https://www.arabidopsis.org/) [50] was employed to get the sequences of the proteins for the seven genes (At3g04080, At5g18280, At1g14240, At1g14230, At1g14250, At2g02970, and At4g19180) of *Arabidopsis thaliana* that belong to the apyrase gene family [2]. On Phytozome v12.1 (https://phytozome.jgi.doe.ov) [51], these sequences were used to run a BLASTp search against the *Oryza sativa* v7 jGI (Rice) dataset. They were also used for the BLASTp search against the NCBI protein database (https://www.ncbi.nlm.nih.gov/protein) and the Rice genome annotation project (http://rice.plantbiology.msu.edu/) [52] separately so that no putative member was missed out. The best hits from these databases were subjected to

domain analysis via InterPro (http://www.ebi.ac.uk/interpro/) [53] to ensure the presence of the GDA1-CD39 domain, which is a characteristic feature of APYs. Entries having this domain were chosen for multiple sequence alignment, which was conducted via MEGA X (Molecular Evolutionary Genetics Analysis) software [54]. Their multiple sequence alignment was visualized via GeneDoc version 2.7 [55] to search for the presence of 5 ACRs [22]. Sequences that contained these 5 ACRs were chosen as members of the apyrase family. To confirm that all members of the apyrase family were included, those sequences were submitted as input sequences for a BLAST analysis in Phytozome [51]. The coding sequence (CDS), genomic, and the peptide sequence of the *OsAPY*s were obtained from Phytozome [51].

Analysis of the physicochemical properties

For assessment of the physicochemical characteristics of the genes, the theoretical isoelectric point (pI), index of instability, grand average of hydropathy (GRAVY), as well as the molecular weight of the proteins were determined. It was done via ProtParam hosted by ExPASy (https://web.expasy.org/protparam/) [56] by uploading the protein sequence. By uploading the protein sequences to WoLF PSORT (https://wolfpsort.hgc.jp/) [57] and CELLO v.2.5 (http://cello.life.nctu.edu.tw/) [58], the subcellular distribution of the proteins was determined.

Analysis of conserved motifs and gene structure

MEME version 5.3.0 (Multiple Em for Motif Elicitation; http://meme-suite.org) [59] was employed to investigate the conserved motifs on proteins in classic mode, and the motif number was determined to be 10. The minimum width was kept to 6, and the maximum one was 50; each motif's highest and lowest sites were set to 600 and 2 accordingly. Depending on the appearance frequency of the motifs in MEME [59], they were numbered sequentially and positioned beside their corresponding OsAPYs according to their phylogenetic groups. In order

to determine their role, each of the ten detected motifs was evaluated via Pfam (http://pfam.xfam.org/) [60].

OsAPY CDS sequences were compared against their respective genomic sequences lacking the UTR (untranslated region) to assess gene structure. Gene structure was determined using the GSDS 2.0 (Gene Structure Display Server) tool (http://gsds.gao-lab.org/) [61], and this web server graphically depicted the gene structure of *OsAPY* genes.

Analysis of phylogenetic relationship

TAIR [50] along with EnsemblPlants (https://plants.ensembl.org) [62] database was employed to get the peptide sequences of *APY*s from *Arabidopsis thaliana* and *Triticum aestivum*, correspondingly. An unrooted phylogenetic tree was created utilizing MEGA X [54]. It was generated using protein sequences from *Oryza sativa*, *Arabidopsis thaliana*, and *Triticum aestivum*. The Jones-Taylor-Thornton (JTT) substitution model was applied with 1000 bootstrap replications using the maximum likelihood method [63] to keep the rates uniform across sites. It was visualized using the web tool iTOL (https://itol.embl.de/) [64].

Prediction of gene duplication

PGDD (Plant genome duplication database) (http://chibba.agtec.uga.edu/duplication/) [65] was employed to examine the gene duplication events and to find out the orthologous and paralogous gene pairs. PGDD [65] provided the Ka (synonymous substitution rate) and Ks (non-synonymous substitution rate) values for the duplicated gene pairs. Using the Ks values and a clockwise rate of synonymous substitution (λ) of 1.5×10^{-8}, the approximate timing of duplication was computed following the formula $T = Ks/2\lambda$ [66]. A circle plot of the paralogous genes was created using TBTools (https://github.com/CJ-Chen/TBtools/releases) [67].

Study of the cis-regulatory elements

The sequence located 1000 bp upstream of *OsAPY*s was retrieved from the genomic sequence of rice using Phytozome [51] for investigating the cis-elements and their function. PlantCARE (http://bioinformatics.psb.ugent.be/webtools/plantcare/htmL/) [68] was utilized for predicting the cis-elements. Cis elements were categorized into different groups, and their functions were identified from the literature review. TBTools [67] was utilized to create a visual description of the cis-regulatory elements.

Analysis of chromosomal distribution

Information from rice genome sequences was used to build a chromosomal organization of *OsAPY* genes based on their location. Phytozome [51] provided details on the number of chromosomes, gene loci, as well as length for the physical map. MapChart (http://www.joinmap.nl) [69] software was used to create a rudimentary physical map of the *OsAPY* gene family, illustrating its location and distribution.

Specification of *OsAPY* targeting miRNAs

For the identification of miRNAs which target *APY* genes in rice, psRNATarget (http://plantgrn.noble.org/psRNATarget/) [70] was used, and it was tested against every mature rice miRNAs present in the database of miRbase [71]. Using Cytoscape (https://cytoscape.org/) [72], the predicted miRNAs were deployed to build a network. To perform the analysis of pre-computed expression of the detected miRNAs, miRid was employed to search against the rice datasets of the PmiRExAt (http://pmirexat.nabi.res.in/) [73] and a heatmap was generated via GraphPad Prism 9.0.0 (https://www.graphpad.com/company/) [74].

Identification of SNPs in *APY* genes

The sequences of *APY* genes from 11 rice varieties with different genotypes based on responses towards abiotic stress [38,75] were compared to the reference Nipponbare sequence using the

Rice SNP-Seek database (https://snp-seek.irri.org/index.zul) [76]. SNPs that could be predominantly attributed to variations in the peptide sequence were recognized throughout the genotypes and were termed single amino acid polymorphisms (SAPs).

Analysis of secondary and tertiary structure of proteins

The secondary structures were generated utilizing the STRIDE program (http://webclu.bio.wzw.tum.de/stride/) [77]. The number and percentage of α helices, extended beta-sheet, turns, coils, and 310-helix were displayed in various colors as part of the structural study. The membrane-spanning motif was investigated by using default parameters of the online tool TMHMM server v.2.0 (http://www.cbs.dtu.dk/services/TMHMM/) [78].

The tertiary structure was generated using the RoseTTAFold method of the Robetta server (https://robetta.bakerlab.org/) [79]. Refinement of the created structures was done via the GalaxyRefine web server (http://galaxy.seoklab.org/refine) [80], and then the energy minimization was done using Swiss-PdbViewer v4.1 (http://www.expasy.org/spdbv/) [81]. PROCHECK (https://servicesn.mbi.ucla.edu/PROCHECK/) [82] and ERRAT (https://servicesn.mbi.ucla.edu/ERRAT/) [83] servers were further used for the validation of the structure. For the assessment of Z-scores and energy plots, ProSA-web (https://prosa.services.came.sbg.ac.at/prosa.php) [84] was utilized. Discovery Studio software was finally used to visualize the tertiary protein structures [85].

Analysis of protein-ligand docking

Molecular docking is an *in-silico* strategy for assessing the binding affinity of a ligand to a receptor molecule. Since ATP is a vital ligand of APY proteins, it was chosen as the ligand for the study. HDOCK server (http://hdock.phys.hust.edu.cn/) [86] was used as the docking tool to conduct the docking analysis between the OsAPY proteins and ATP. It was done using the

default parameters. The 3D structure of ATP was downloaded from the PubChem database (PubChem CID: 5957). After docking, the top 10 solution complex generated via HDOCK [86] were downloaded, and their structures were further analyzed and validated using PDBsum (http://www.biochem.ucl.ac.uk/bsm/pdbsum) [87], PROCHECK [82] and ERRAT [83] servers. The best structure was selected, and it was aligned and visualized. Then finally, the protein and ligand residue interaction was studied using Discovery Studio [85].

Study of expression profiling of *OsAPY*s in rice using RNA-seq data

Rice Genome Annotation Project [52] was utilized to collect the data for the expression of *APY* genes under several tissues. Accordingly, the RNA-seq expression values were listed. GraphPad Prism 9.0.0 [74] software was used to create a heat map from the data. GENEVESTIGATOR (https://genevestigator.com/gv/) [88] provided the pattern of *OsAPY* expression in various stresses, and the log2 values of relative expression were used to generate the heat map via GraphPad Prism 9.0.0 [74].

Plant germination, treatment, and total RNA isolation

The healthy, high-quality and mature seeds of BRRI dhan28 were obtained from the Bangladesh Rice Research Institute (BRRI) and used in this experiment. They were washed thoroughly and then were allowed to germinate on a petri dish containing water-soaked tissue paper. After 3-4 days, the germinated seedlings were transferred to the hydroponic culture system. A controlled condition was maintained in the culture room, including a temperature of 25±2 °C with a photoperiod consisting of 16 hours of light followed by 8 hours of darkness and 1500-2000 lux light intensity. After 20 days, the seedlings were subjected to different stresses for 18-20 hours which included cadmium stress (100mM $CdCl_2$ dissolved in distilled water), cold (4 °C), salinity (100mM NaCl dissolved in distilled water), submergence, drought

(3 mg/L polyethylene glycol dissolved in distilled water), heat stress (42 °C). As control, seedlings that had been untreated were utilized. After the treatment, fresh young leaves were collected and washed several times with 70% alcohol and distilled water in order to extract the RNA. Using Invitrogen™ TriZOL™ reagent (Thermo Fisher Scientific Corporation, USA), total RNA was isolated from leaves. The extracted RNA was subsequently processed with DNase I of Invitrogen™ DNA-free™ DNA Removal Kit (Thermo Fisher Scientific Corporation, USA) to remove the genomic DNA contamination. Finally, the GoScript™ Reverse Transcription System (Promega Corporation, USA) was utilized to synthesize the complementary DNA (cDNA). These procedures were carried out per the protocol of the manufacturers.

Analysis of gene expression under abiotic stress conditions using RT-qPCR data

Primer3 v.0.4.0 (https://bioinfo.ut.ee/primer3-0.4.0/) [89] was used to generate primers for the RT-qPCR, keeping the product length between 208 and 220 bp. The real-time PCR was done using GoTaq® qPCR Master Mix (2X) (Promega Corporation, USA) on CFX96™ Real-Time PCR Detection System (BioRad). For the reference gene, eukaryotic elongation factor 1 alpha (*eEF-1α*) was chosen [90]. Each set of gene-specific primers took up 1 µL of the 15 µL reaction mixture, which also comprised 7.5 µL of GoTaq® qPCR Master Mix (2X), 2 µL of cDNA (10 times diluted), and 3.5 µL of nuclease-free water. In order to carry out each of the reactions, the following conditions were applied: at 95 °C initial denaturation for 10 min preceding 40 cycles of denaturation at 95 °C for 15s, annealing for 30s, and extension at 72° C for 40s. The annealing temperature was 55.4 °C for *OsAPY2* and *OsAPY4*; 56.4 °C for *OsAPY1* and *OsAPY5*; 57.4 °C for *OsAPY3*, *OsAPY6*, and *OsAPY8*; 58.4 °C for *OsAPY7* and *OsAPY9*; 55.7 °C for *eEF-1α*. Three separate experiments were carried out for each sample and the melting

curve analysis was done after the PCR amplification. The delta-delta Ct value approach [91] was utilized in calculating the ratio of relative expression. Technical replication was used to find the mean value of expression at different treatments. MS Office 365 and GraphPad Prism 9.0.0 [74] were used to analyze the data. A one-way ANOVA, followed by a Bonferroni post hoc test, was used to assess the significant differences ($P \leq 0.05$). To represent the significant differences, different means were labeled with different number of stars (*).

Results

Identification of *APY* family members in rice and study of their physicochemical properties

Rice was found to contain nine members of the *APY* gene family. To BLAST against the rice genome, the *Arabidopsis APY*s were utilized as reference sequences. Upon performing BLASTp searches against the *Oryza sativa*, a total of 19 hits were found containing the GDA1-CD39 domain. All the domain annotations were confirmed by sequence analysis in InterPro [53].

These 19 transcripts belonged to a total of 12 genes. The primary transcripts annotated by Phytozome [51] were selected as the representative transcripts of the genes with alternative splice forms. 9 of the 12 genes were found to possess all five Apyrase Conserved Regions (ACRs) (S1 Fig); hence they were designated Apyrase genes. For the naming of the genes (*OsAPY1*-*OsAPY9*), the prefix 'Os' for *Oryza sativa* was used, followed by 'APY' for Apyrase, and then the sequential number that corresponded to their chromosome number and location was used. Table 1 lists the physicochemical properties of all representatives of the *OsAPY* Family.

303 **Table 1. Physicochemical properties of the members of the apyrase gene family in rice**

304 **(*O. sativa*).**

Gene Name	Locus Name	Length			MW (Da)	pI	Instability Index	GRAVY Value	Localization
		Genomic (bp)	CDS (bp)	Protein (aa)					
OsAPY1	LOC_Os03g21120	5548	1470	489	52799.01	5.72	39.76 (Stable)	-0.09	Cp[ab]
OsAPY2	LOC_Os03g26080	3847	1527	508	55346.06	9.1	53.33 (Unstable)	-0.204	PM[ab]
OsAPY3	LOC_Os07g48430	4260	1404	467	50437.74	8.97	36.76 (Stable)	-0.136	Mt[a], Cp[b]
OsAPY4	LOC_Os08g33850	4217	1629	542	59596.12	9.34	48.76 (Unstable)	-0.149	PM[a], ER[b]
OsAPY5	LOC_Os10g21000	4624	2109	702	77242.54	9.18	43.81 (Unstable)	-0.171	PM[ab]
OsAPY6	LOC_Os11g03270	6059	1647	548	59542.4	7.96	36.68 (Stable)	-0.077	Cp[ab]
OsAPY7	LOC_Os11g03290	3902	1374	457	49622.22	5.44	31.59 (Stable)	-0.179	Cp[ab]
OsAPY8	LOC_Os11g25260	7876	1428	475	50321.86	5.83	37.31 (Stable)	-0.12	Cp[ab]
OsAPY9	LOC_Os12g02980	3138	1356	451	48900.8	8.01	30.98 (Stable)	-0.155	Cp[a], ER[b]

305 CDS- Coding sequence, MW- Molecular weight, pI- Isoelectric point, GRAVY- Grand average

306 of hydropathy, Cp- Chloroplast. PM- Plasma membrane, Mt- Mitochondria, ER- Endoplasmic

307 reticulum.

308 [a]Subcellular localization according to CELLO, [b]subcellular localization according to WoLF

309 PSORT.

310

The theoretical pI of proteins belonging to the apyrase gene family ranged between 5.44 and 9.34, with an average of 7.73. *OsAPY*4 had the highest and *OsAPY*7 had the lowest pI value. The proteins had molecular weights ranging from 48900.8 Da to 77242.54 Da belonging to *OsAPY*9 and *OsAPY*5, respectively. The average molecular weight of the proteins was 55978.8 Da. The GRAVY value for all the proteins was negative, and as per the data, all protein molecules are hydrophilic [92]. Six genes had an instability index lower than 40, meaning they are stable. It revealed that 67% of the genes are stable, and 33% of them are unstable.

For the prediction of subcellular location, two different tools were used, and per the subcellular localization, both ecto- and endo-APYs are present in this gene family [23]. Their results varied in OsAPY3, OsAPY4, and OsAPY9. According to CELLO [58], they are located on mitochondria, plasma membrane, and chloroplast. On the other hand, according to WoLF PSORT [57], their subcellular localization is on chloroplast for OsAPY3 and endoplasmic reticulum for OsAPY4 and OsAPY9. The predicted subcellular localization of the proteins according to two different tools is given in Table 1.

Analysis of conserved motifs and gene structure

In total, ten conserved motifs were discovered, which were numbered 1-10 (Fig 1b). 4 motifs, including motif 1, 5, 8, and 10, were conserved and existed in all the OsAPYs. Members of each phylogenetic group had similar motif distribution, which affirms the classification of groups. All the members of group I in the phylogenetic tree (Fig 1a) had the same motif distribution, containing all the ten motifs. On the other hand, the members of group II in the phylogenetic tree, OsAPY2, and OsAPY4, contained almost similar numbers of motifs except motif 2, which was present in OsAPY4 only. Though only OsAPY5 belonged to group III, its motif distribution was the same as OsAPY4 despite being in different phylogenetic groups. Functions of these motifs were also analyzed, but there was no information on the function of

motif 9 and 10. Their analysis revealed that the remaining eight motifs belong to the GDA1/CD39 (nucleoside phosphatase) family (S1 Table).

Fig 1. Schematic depiction of phylogenetic relationship, gene structure, and conserved motifs of *APY* genes. a- Phylogenetic relationship among *OsAPY*s generated via maximum likelihood approach. The green, pink and blue boxes represent groups I, II, and III, respectively. b- OsAPY conserved motif distribution. Ten varying-colored boxes represent the motifs. The legend below shows the corresponding motif's protein sequence. c- Gene structure of *APY*s. Yellow color boxes specify exons, and introns are depicted by lines. The exon-intron lengths can be calculated following the scale shown below.

The exon and intron arrangement of *OsAPY*s was studied in order to better comprehend their structure. The total number of coding sequences (CDS) or exons and introns of the *OsAPY* genes were 2-12 and 1-11, respectively (Fig 1c), and there was no intronless gene. *OsAPY5* contained the lowest number of exons and introns, which are two exons and one intron, and on the other hand, *OsAPY6* contained the highest number of exons and introns, which is 12 exons and 11 introns.

Analysis of phylogenetic relationship in *OsAPY* family

The maximum likelihood method was utilized to create an unrooted phylogenetic tree to study the evolutionary relationship between the *APY* genes. It was done using the peptide sequences of seven apyrase homologs from *Arabidopsis thaliana* (*AtAPY*) [2], nine apyrase homologs from *Triticum aestivum* (*TaAPY*) [23] and the nine identified apyrase homologs from *Oryza sativa* (*OsAPY*). It was demonstrated by this phylogenetic tree (Fig 2) that the nine *OsAPY* genes could be split into three separate groups referred to as I, II, and III. There were already three distinct groups for the *AtAPY* and *TaAPY* genes [23]. No *OsAPY* gene was classified into the new group. Among the 9 *OsAPY* genes, *OsAPY1, OsAPY3, OsAPY6-OsAPY9* belonged to

group I. *TaAPY1-TaAPY3.4* and *AtAPY1*, *AtAPY2* also were in group I. *OsAPY2*, and *OsAPY4* fell in group II. Group II also contained *TaAPY5*, *TaAPY6*, *AtAPY3-AtAPY6*. Group III consisted of *OsAPY5*, *AtAPY7*, and *TaAPY7*.

Fig 2. Phylogenetic analysis of the *APY*s in rice, *Arabidopsis*, and wheat. The MEGA X software was employed to generate a phylogenetic tree by utilizing the maximum likelihood approach along with 1000 bootstrap replications. Genes were divided into three different groups, each marked with a different color.

Analysis of gene duplication

A crucial role is played by duplication events for expanding the gene family and in the emergence of new gene functions. There were six duplications in total in the rice genome, with three occurring within the *APY* family (Fig 3 and S2 Table). Because no genes on the same chromosome had been duplicated, there was no tandem duplication at all. In this study, the duplication type was segmental. The three groups of segmentally duplicated genes within the rice apyrase gene family are *OsAPY1/9*, located on chromosomes 3 and 12, respectively; *OsAPY1/3*, found on chromosomes 3 and 7, respectively; *OsAPY3/9*, situated on chromosomes 7 and 12 respectively.

Fig 3. Duplication events of *OsAPY*s within rice genome. Duplication of the *OsAPY*s was specified by the red lines, and the one among the whole rice genome was denoted by the gray lines. TBTools was used to create the circle plot.

The non-synonymous (Ka) and synonymous (Ks) substitution rate of genes was used to measure the selection pressure of duplication occurrences. Ka/Ks = 1 implies neutral selection, whereas Ka/Ks<1 represents purifying selection, and Ka/Ks>1 denotes positive selection [93]. Between 0.1476 to 0.5560, Ka/Ks of segmental duplication had a mean of 0.28021. As demonstrated by Ka/Ks ratios lower than 1, all the genes originated under the influence of

purifying selection (S2 Table). The duplication time of each event was counted in million years ago (MYA) unit (S2 Table), and it occurred between 66.6 MYA and 1.54 MYA.

Eight orthologous pairs were found between rice *OsAPY*s and other species (Table 2). It- is duplicated with sorghum, western poplar, cotton, grapevine, maize, and soybean. The range of Ka/Ks was between 0.143 and 0.357, and the mean was 0.2471. These data suggest that duplication events had a significant impact on the expansion and functional diversity, and an important role was served by segmental duplication in the evolution of the *APY* family of genes.

Table 2. Duplication event between rice *APY* genes and other species.

Duplicated Gene 1	Duplicated Gene 2	Ka	Ks	Ka/Ks	Duplication time (MYA)	Purifying Selection	Duplication type
OsAPY2	Sobic.001G356200 (Sorghum)	0.1427	0.4936	0.2891	16.45	Yes	Segmental
OsAPY1	Potri.019G031000 (Western Poplar)	0.2653	1.6902	0.157	56.34	Yes	Segmental
OsAPY1	Gorai.007G268200 (Cotton)	0.3114	1.6822	0.1851	56.07	Yes	Segmental
OsAPY2	GRMZM2G056944 (Maize)	0.16	0.4481	0.3571	14.93	Yes	Segmental
OsAPY2	GRMZM2G097987 (Maize)	0.158	0.4801	0.3291	16	Yes	Segmental
OsAPY4	Glyma.02G107700 (Soybean)	0.4302	1.6258	0.2646	54.19	Yes	Segmental
OsAPY4	Glyma.01G047100 (Soybean)	0.4293	1.7026	0.2521	56.75	Yes	Segmental

OsAPY4	GSVIVT01019977001 (Grape vine)	0.3133	2.1857	0.1433	72.85	Yes	Segmental

391

392 Cis-acting regulatory elements (CAREs) analysis

393 Rice *APY* genes might be regulated by promoter sequences, which are known to be associated
394 with the regulation of transcription of the genes in plants. Analysis of 1 kbp upstream promoter
395 sequences in *O. sativa* indicated the presence of 69 CAREs. These cis-elements were grouped
396 into eight different functional categories (Fig 4): i) Light responsive cis-elements, ii) Abiotic
397 challenge responsive elements, iii) Hormonal regulation responsive elements, iv) Elements
398 responsible for cellular development, v) Promoter associated elements, vi) Biotic challenge
399 responsive elements, vii) Elements with miscellaneous functions and viii) Elements with
400 unknown functions. Hormonal regulation responsive elements were further divided into a)
401 MeJA responsive, b) Salicylic acid-responsive, c) Auxin responsive, d) Gibberellin responsive,
402 e) Ethylene responsive, and f) Abscisic acid-responsive elements (Fig 4).

403 **Fig 4. Schematic diagram of predicted cis-elements in *OsAPY* promoter region.** Upstream
404 nucleotides of the translation initiation point are shown by the scale at the end. Different
405 colored boxes depict different cis-regulatory elements.

406 Different abiotic stress-associated elements (anaerobic, anoxic, low temperature, drought, salt,
407 and cold) were observed in the *OsAPY* promoter region (Table 3). STRE, TC-rich repeats,
408 MBS, ARE, GC-motif, LTR, CCAAT-box, AP-1, DRE core, MYB, MYC, were the abiotic
409 challenge responsive cis-elements. Among all these elements, STRE was present in the highest
410 frequency, and DRE1 was present in the lowest frequency. W box, WRE3, and WUN-motif
411 (Table 3), the biotic challenge responsive elements, mainly act as fungal elicitors and wound-

412 responsive elements. WRE3 occurred in the highest frequency, and WUN-motif occurred in
413 the lowest frequency.

414 **Table 3. List of cis-regulatory elements (CREs) found in the 5′ UTR region of the**
415 ***OsAPY*s.**

Responsive factors	CREs	Function	Reference(s)
Hormonal regulation responsive	ABRE	Involved in the abscisic acid responsiveness	[94]
	ABRE3a	Involved in the abscisic acid responsiveness	[95]
	ABRE4	Involved in the abscisic acid responsiveness	[95]
	GARE-motif	Gibberellin-responsive element	[96,97]
	P-box	Gibberellin-responsive element	[98]
	TCA	Involved in salicylic acid responsiveness	[23]
	TCA-element	Involved in salicylic acid responsiveness	[98,99]
	TGA-element	Auxin-responsive element	[100]
	CARE	Enhances the level of gibberellin (GA) -induced expression	[101]
	CGTCA-motif	Involved in the Methyl Jasmonate (MeJA)-responsiveness	[100]
	TGACG-motif	Involved in the MeJA-responsiveness	[102]
	ERE	Ethylene-responsive element	[98]
	as-1	Involved in the MeJA-responsiveness	[103]
	box S	Regulate jasmonate- and elicitor-responsive expression	[104]
Cellular development	CAT-box	Related to meristem expression	[105]
	HD-Zip 1	Involved in differentiation of the palisade mesophyll cells	[106]

	circadian	Involved in circadian control	[106,107]
	RY-element	Involved in seed-specific regulation	[108]
	O2-site	Involved in zein metabolism regulation	[100]
	CCGTCC motif	Meristem specific activation	[109]
	CCGTCC-box	Meristem specific activation	[110]
	AAGAA-motif	Involved in secondary xylem development	[111]
	AC-II	Involved in xylem specific expression.	[112]
Light responsive	3-AF1 binding site	Light responsive element	[96]
	AE-box	Part of a module for light response	[98]
	ATCT-motif	Part of a conserved DNA module involved in light responsiveness	[97]
	Box 4	Part of a conserved DNA module involved in light responsiveness	[113]
	G-Box	Involved in light responsiveness	[98]
	G-box	Involved in light responsiveness	[100]
	GA-motif	Part of a light responsive element	[114]
	GATA-motif	Part of a light responsive element	[115]
	GT1-motif	Light responsive element	[116]
	Gap-box	Part of a light responsive element	[117]
	I-box	Part of a light responsive element	[113,118]
	L-box	Part of a light responsive element	[115]
	MRE	MYB binding site involved in light responsiveness	[115]
	Sp1	Light responsive element	[115]

	TCCC-motif	Part of a light responsive element	[119]
	TCT-motif	Part of a light responsive element	[120]
Abiotic challenge responsive	AP-1	Stress responsive cis-element	[121]
	ARE	Essential for the anaerobic induction	[112]
	GC-motif	Enhancer-like element involved in anoxic specific inducibility	[121]
	LTR	Involved in low-temperature responsiveness	[100]
	MBS	MYB binding site involved in drought-inducibility	[123]
	TC-rich repeats	Involved in defense and stress responsiveness	[100]
	CCAAT-box	MYBHv1 binding site	[124]
	DRE core	Regulation of drought, high-salt, and cold stresses	[125]
	MYB	Involved in drought, low temperature, salt and ABA stress responses	[126,127]
	MYB recognition site	Involved in the drought-induced expression	[126]
	MYC	Involved in early response to drought and abscisic acid induction	[128]
	STRE	Involved in defense and stress responsiveness	[122]
Biotic challenge responsive	W box	Fungal elicitor responsive element	[129]
	WRE3	Wound-responsive element	[122]
	WUN-motif	Wound-responsive element	[129]

Promoter-related elements	CAAT-box	Common cis-acting element in promoter and enhancer regions	[100]
	TATA-box	Core promoter element around -30 of transcription start	[100]
Miscellaneous	3-AF3 binding site	Part of a conserved DNA module array (CMA3)	[130]
	AT-rich sequence	Binding site of AT-rich DNA binding protein (ATBP-1)	[100]
	Box III	Protein binding site	[115]
	Myb-binding site	Myb-binding site	[131]
	MYB-like sequence	MYB recognition sequence	[131]

TGACG motif, CGTCA motif, TGA element, TCA element, GARE-motif, ABRE, P-box, ERE, as-1, and box S constituted the hormonal regulation responsive cis-elements (Table 3). Cellular development responsive cis-elements play a major role in the meristem expression, palisade mesophyll tissue differentiation, circadian control, seed-specific regulation, zein metabolism regulation, and xylem-specific expression (Table 3). These cis-elements included CAT-box, HD-Zip 1, circadian, RY-element, O2-site, CCGTCC motif, CCGTCC box, AAGAA-motif, and AC-II.

Light responsive cis-elements included 3-AF1 binding site, TCT-motif, TCCC-motif, MRE, Gap-box, I-box, GT1-motif, ATCT-motif, Box 4, GATA-motif, GA-motif, G-box, G-Box, AE-box, L-box, Sp1, (Table 3). They mainly function as a light responsive element or a module or a component of such an element. TATA-box and CAAT-box were the two elements, related to promoter, found in *OsAPY* genes, and they are core promoter elements that mainly function in

promoter and enhancer regions. Cis-elements with miscellaneous functions included 3-AF3 binding site, MYB-like sequence Myb-binding site, Box III, and AT-rich sequence (Table 3). *OsAPY5* contains a 3-AF3 binding site that is a DNA module array component. The AT-rich DNA binding protein (ATBP-1) utilizes a binding site situated on *OsAPY7*, which is located on the AT-rich sequence. On the other hand, Box III is located on *OsAPY7* as a binding site for proteins.

Analysis of chromosomal distribution

All the 12 chromosomes of rice were examined for *APY* gene distribution, and the results indicated an unequal distribution of *APY* genes (Fig 5). No *OsAPY* member was mapped onto chromosome 1, 2, 4, 5, 6, and 9. It was observed that both *OsAPY1* and *OsAPY2* were on chromosome 3. The chromosomal positions of *OsAPY3*, *4*, *5*, and *9* were 7, 8, 10, and 12, respectively. *OsAPY6*-*OsAPY8* was located on chromosome 11. *OsAPY1*, *2*, *5*, and *8* were concentrated near the centromere. *OsAPY6*, *7*, and *9* were situated on the p arm of the chromosome, and on the other hand, *OsAPY3* and *4* were placed on the q arm of the chromosome. The location of all the *OsAPY*s in different chromosomes, their position, and orientation are mentioned in the S3 Table.

Fig 5. Distribution of *OsAPY*s throughout the rice genome. The figure was generated using MapChart. Chromosome number is presented on top. C depicts the centromere position. The position of every gene can be easily compared following the reference chromosome at the left.

Identification of miRNAs targeting *OsAPY* genes

In this study, 103 potential, as well as unique miRNAs of 19–24 nucleotides in length, were found to target the *OsAPY* family members in rice. The highest number of miRNAs targeted *OsAPY9*, and *OsAPY3* was targeted by the lowest number. Fig 6 illustrates the regulatory

452 relationships involving potential miRNAs as well as their targeted *APY*s. The majority of the
453 miRNAs expected to target *OsAPY*s have a strong inhibitory effect through cleavage. The
454 inhibitory action for only a few numbers of miRNAs was translation. The list of miRNAs
455 targeting different *OsAPY*s and their mode of inhibition is given in the S4 Table.

456 **Fig 6. Identification of potential miRNAs targeting *OsAPY* genes.** Visual depiction of
457 miRNA-*OsAPY* interaction is generated via Cytoscape. Arrows depict the regulatory
458 relationship, elliptical shapes of different colors represent the *OsAPY*s, and the miRNAs are
459 shown in ash-colored boxes.

460 Among all the miRNAs, 23 miRNAs targeted more than one *OsAPY*s, and the rest were unique
461 for each gene. It was found that most of the miRNAs had lower expression patterns. A heat
462 map was generated (Fig 7) by comparing miRNA expression levels from PmiRExAt [73]
463 across tissues and under a number of different abiotic stress conditions. Among all the
464 miRNAs, osa-miR159a.1 targeting *OsAPY4* was expressed highly in all stresses and tissues
465 except anther and leaves during the flowering stage. The target of osa-miR5532 was *OsAPY2*
466 and *OsAPY5*, which was abundantly expressed in anther. osa-miR3979-3p, which targeted
467 *OsAPY4*, was strongly expressed in roots. osa-miR408-3p targeting *OsAPY5*, *9*, was highly
468 expressed in leaves during the flowering stage and in seedlings exposed to H_2O_2. These
469 expressions of most of the miRNAs were downregulated during different stresses suggesting
470 the increased expression of the *OsAPY*s in such stress conditions. Therefore, sequence-specific
471 miRNA-mediated interaction may have a vital function in regulating *OsAPY* genes, which in
472 turn may help plants act on environmental as well as growth signals.

473 **Fig 7. Analysis of *APY*-targeting miRNA expression in different abiotic stresses and**
474 **tissues.** The expression profile of each miRNA can be analyzed following the scale at the right.
475 A heat map was generated using GraphPad Prism 9.0.0.

Study of SNPs in *OsAPY*s

Rice SNP-Seek database [76] was used to better understand the variations in alleles of *OsAPY* members throughout 11 rice varieties and were selected based on their stress responses. It allowed identifying the Single Amino acid Polymorphisms (SAPs) (Table 4). SAPs were identified in 6 *OsAPY*s, but not in *OsAPY1*, *5*, and *8*. It indicates that the genes of *OsAPY1*, *5*, and *8* are substantially conserved among rice genotypes. The indica varieties include NERICA-L-27, Pokkali, Rasi, Vandana, Swarna, and IR-64, while Azucena and NERICA-1 are tropical japonica varieties. GIZA 159, Nagina 22, and Pusa (Basmati 1) are the members of the temperate japonica, aus, and unassigned variety, respectively. The study revealed that indica rice varieties have a higher rate of SAPs than other rice varieties. 5 SAPs were identified in *OsAPY2*; *OsAPY3*, *7*, and *9* showed 3 SAPs, while *OsAPY4* had only one SAP, but *OsAPY6* contained 4 SAPs.

488

489 **Table 4. Distribution of single amino acid polymorphisms (SAPs) throughout the *APY*s**

490 **of chosen rice varieties.**

Gene Name	Nipponbare	Pokkali	Rasi	IR-64	NERICA-L-27	Pusa (Basmati 1)	Swarna	Vandana	NERICA-1	Nagina 22	Azucena	GIZA 159
OsAPY2	A_{109}	A_{109}	A_{109}	A_{109}	A_{109}	A_{109}	V_{109}	A_{109}	A_{109}	A_{109}	A_{109}	A_{109}
	R_{258}	R_{258}	R_{258}	R_{258}	R_{258}	R_{258}	R_{258}	R_{258}	R_{258}	R_{258}	R_{258}	H_{258}
	K_{295}	K_{295}	K_{295}	K_{295}	K_{295}	K_{295}	K_{295}	K_{295}	K_{295}	N_{295}	K_{295}	K_{295}
	S_{365}	A_{365}	A_{365}	S_{365}	S_{365}	S_{365}	A_{365}	A_{365}	A_{365}	S_{365}	S_{365}	S_{365}
	K_{388}	Q_{388}	Q_{388}	Q_{388}	Q_{388}	Q_{388}	Q_{388}	Q_{388}	Q_{388}	Q_{388}	K_{388}	K_{388}
OsAPY3	E_{111}	A_{111}	A_{111}	A_{111}	A_{111}	A_{111}	A_{111}	A_{111}	E_{111}	A_{111}	-	E_{111}
	N_{114}	K_{114}	K_{114}	K_{114}	K_{114}	K_{114}	K_{114}	K_{114}	N_{114}	K_{114}	N_{114}	N_{114}
	V_{136}	A_{136}	A_{136}	A_{136}	A_{136}	A_{136}	A_{136}	A_{136}	V_{136}	A_{136}	V_{136}	V_{136}
OsAPY4	S_{207}	G_{207}	G_{207}	G_{207}	G_{207}	G_{207}	G_{207}	G_{207}	G_{207} S_{207}	G_{207}	G_{207}	S_{207}
OsAPY6	M_{77}	K_{77}	K_{77}	K_{77}	K_{77}	K_{77}	K_{77}	K_{77}	M_{77}	-	M_{77}	M_{77}
	I_{162}	R_{162}	R_{162}	R_{162}	R_{162}	R_{162}	R_{162}	R_{162}	I_{162}	R_{162}	I_{162}	I_{162}
	P_{252}	S_{252}	S_{252}	S_{252}	-	S_{252}	S_{252}	S_{252}	P_{252}	S_{252}	P_{252}	P_{252}
	E_{261}	K_{261}	K_{261}	K_{261}	K_{261}	K_{261}	K_{261}	K_{261}	E_{261}	K_{261}	E_{261}	E_{261}
OsAPY7	I_{236}	T_{236}	T_{236}	T_{236}	T_{236}	T_{236}	T_{236}	T_{236}	I_{236}	T_{236}	I_{236}	I_{236}
	E_{242}	G_{242}	G_{242}	G_{242}	G_{242}	G_{242}	G_{242}	G_{242}	E_{242}	G_{242}	E_{242}	E_{242}

	V_{264}	V_{264}	V_{264}	V_{264}	V_{264}	V_{264}	V_{264}	V_{264}	I_{264}	V_{264}	V_{264}	V_{264}
OsAPY9	N_{75}	N_{75}	D_{75}	N_{75}	N_{75}	N_{75}	N_{75}	N_{75}	N_{75}	D_{75}	N_{75}	N_{75}
	Q_{290}	H_{290}	Q_{290}	H_{290}	H_{290}	H_{290}	H_{290}	H_{290}	H_{290}	Q_{290}	H_{290}	Q_{290}
	N_{350}	N_{350}	D_{350}	N_{350}	N_{350}	N_{350}	N_{350}	N_{350}	N_{350}	D_{350}	N_{350}	N_{350}

- Represent the polymorphism in the non-coding region.

Analysis of secondary and tertiary structure

The secondary structure analysis revealed the position of alpha-helix, beta-sheet, isolated beta bridge, turn, coil, 310-helix, and transmembrane helix (Fig 8). Their percentage and the position of the transmembrane helix are given in the S5 Table. It revealed that alpha-helix is dominant over all the other secondary structures, followed by the turn, beta-sheet, coil, and 310-helix. There were some exceptions in OsAPY2, 4, 5, and 8. In OsAPY5, the coil percentage is higher than the beta-sheet, and in OsAPY2, it is higher than the turn and beta-sheet. In OsAPY4 and OsAPY8, the beta-sheet percentage is higher than that of turn. The higher percentage of helix and beta-sheet indicate the stability of the OsAPYs [132], and the structures like random coils are critical for the signaling cascades [133]. The analysis of the motifs spanning the membrane (MSM) indicated that 4 OsAPYs contained one membrane-spanning motif (MSM), 4 OsAPYs contained 2 MSMs, and 1 OsAPY contained no MSM. OsAPY1, 3, 7, 8 contained only one membrane-spanning motif at N-terminal. OsAPY2, 4, 5, and 6 had two MSMs positioned at the N- and C-terminals separately except OsAPY6, where both the MSMs were located on N-terminal. On the other hand, OsAPY9 contained no MSM.

Fig 8. Secondary structure analysis of the nine rice APYs. Secondary structures were generated using the STRIDE program, and the corresponding positions of membrane-spanning

motifs were identified via the TMHMM server. The cross-membrane domains were marked with a black colored box. Legend at the bottom-right side, shows the icon foe each secondary structure.

RoseTTAFold, a deep learning-based modeling approach, was applied to construct 3D models of proteins using the Robetta web server [79]. The generated models were further refined by GalaxyRefine [80], and then the energy minimization was done via Swiss-PdbViewer [81]. Fig 9 illustrates the modeled tertiary structures of all the OsAPY proteins, visualized via Discovery Studio. These generated structures were then subjected to validation analysis utilizing PROCHECK [82], ERRAT [83], and ProSA-web server [84] (S6 Table). Ramachandran plot analysis in PROCHECK was used to evaluate protein quality [82]. In the favored and additional allowed regions, over 90% of the residues were located, with only <1.5% in the disallowed regions, which confirmed that the projected models are of good quality (S2 Fig). The proteins exhibited an overall quality factor of >87, according to ERRAT [83] analysis (S3 Fig). ProSA-web [84] revealed the Z-score, the level of nativeness of the designed models (S6 Table)**,** and the energy plot, which shows the local quality of the models. The Z-score was found to be in the spectrum of values generally reported for native proteins, implying higher quality of the structures generated, and the models were well within the range of X-ray crystal structure (S4 Fig). As per the energy plot (S5 Fig), all the residues in the simulated structure had a lower value of energy. These findings indicate the excellent quality of the tertiary structures of modeled proteins.

Fig 9. Tertiary structure analysis of the nine rice APYs. The online tool Robetta was used to construct the tertiary structure, and these structures were visualized via Biovia Discovery Studio Visualizer.

Analysis of molecular docking

534 ATP, a vital ligand of APY proteins, was chosen for the analysis of docked protein-ligand
535 complex. The docking analysis was done using the HDOCK server, and it revealed that the
536 docking score of the protein and ATP was between -199.05 and -152.53 (S7 Table). This
537 optimal docking indicated an excellent binding affinity. According to PDBSum [87] analysis,
538 the protein and ATP complex contained 3 to 11 hydrogen bonds (S8 Table). The interaction
539 between the protein and ATP visualized via Discovery Studio [85] revealed the presence of
540 different types of H-bond, electrostatic bond, and hydrophobic bonds (Fig 10 and S9 Table).
541 Validation of the protein-ligand complex via PROCHECK and ERRAT suggested the high
542 quality of the complexes (S6 and S7 Figs).

543 **Fig 10. Protein-ligand residual interaction analysis of OsAPYs with ATP depicted by**
544 **aqua and red color, respectively.** Illustration of bonds: carbon-hydrogen bonds- snowy mint
545 lines, conventional hydrogen bonds- green lines, pi-cation bonds- black lines, unfavorable
546 bumps- red lines, unfavorable negative-negative interactions- yellow lines, attractive charge
547 interactions- orange lines, pi-donor hydrogen bonds- deep brown lines, pi-sigma bonds- light
548 purple lines, unfavorable acceptor- acceptor interactions- navy blue lines, pi-alkyl bonds-
549 magenta lines, unfavorable donor-donor interactions- pink lines, pi-anion bonds- deep-sea blue
550 lines, pi-lone pair interactions- lemon green lines, salt bridge- purple lines.
551 OsAPY1 formed seven conventional hydrogen bonds, 2 Pi-cation interactions, and seven
552 unfavorable interactions (Fig 10). Among all the protein residues, THR168 formed 2 of the
553 seven hydrogen bonds, and ARG99 formed both the Pi-cation interactions (S9 Table). OsAPY2
554 had one attractive charge interaction, 1 Pi-donor hydrogen bond, six conventional hydrogen
555 bonds, five unfavorable interactions, six carbon-hydrogen bonds, and 1 Pi-sigma interaction
556 with ATP. OsAPY3 made one attractive charge interaction, three Pi-alkyl bonds, carbon-
557 hydrogen bonds, two unfavorable interactions, and nine conventional hydrogen bonds.
558 OsAPY4 created four conventional hydrogen bonds, 2 Pi-donor hydrogen bonds, and two

559 carbon-hydrogen bonds. OsAPY5 formed ten carbon-hydrogen bonds, six conventional
560 hydrogen bonds, 1 Pi-lone pair interaction, 2 Pi-anion interactions, and seven unfavorable
561 interactions. OsAPY6 made 2 Pi-cation interactions, Pi-donor hydrogen bonds, carbon-
562 hydrogen bonds, Pi-anion interactions, four conventional hydrogen bonds, four attractive
563 charge interactions, and 1 Pi-alkyl interaction. OsAPY7 and OsAPY8 formed 9 and 12
564 interactions with ATP, respectively. OsAPY9 had one salt bridge interaction, two attractive
565 charge interactions, seven conventional hydrogen bonds, 2 Pi-cation interactions, 1 Pi-anion
566 interaction, 1 Pi-alkyl interaction, and eight unfavorable interactions. These bonds between the
567 OsAPYs and ATP indicate a strong docking interaction.

568 Investigation of the expression profiles of *OsAPY* genes using RNA-
569 seq data

570 Using RNA transcript profiling to analyze the gene expression is an efficient technique. To
571 better comprehend the expression profile of *OsAPY*s, the RNA-seq data was utilized under
572 several tissue types and stresses (Fig 11). The Rice Genome Annotation Project [52] provided
573 RNA-seq data for *OsAPY* expression profiling in several tissues which was used to produce a
574 heatmap (Fig 11).

575 **Fig 11. Heatmap of the expression pattern of the *OsAPY* genes according to tissue type.**
576 The RNA-seq data collected from the Rice Genome Annotation Project was used to conduct
577 expression analysis. The heat map was generated using GraphPad Prism 9.0.0. Expression
578 profile can be analyzed following the bottom located scale. The red boxes represent high
579 expression rates, greens depict low expression rates, and black boxes signify moderate
580 expression levels.

581 The analysis revealed that the expression was higher in the inflorescence, seed, pistil, embryo,
582 and endosperm. *OsAPY1* and *3* upregulated in most of these tissues, whereas in the pre-

583 emergence inflorescence and anther, *OsAPY2* and *4* upregulated. *OsAPY4* was expressed
584 highly in the pistil. For *OsAPY5*, it was higher in pistil, seed, embryo, and endosperm among
585 these tissues. Some of these showed an expression pattern that was tissue-specific, including
586 *OsAPY2*, upregulated in anther, inflorescence, and downregulated in the other types of tissues.
587 In the same manner, the expression of *OsAPY8* was high in shoots. All the *OsAPY*s were
588 downregulated in leaves, post-emergence inflorescence, and seedlings except *OsAPY9*, which
589 was upregulated in these tissues. In shoot tissue, *OsAPY*3 and *8* were highly expressed; on the
590 other hand, *OsAPY3* and *5* were upregulated in callus, and it was *OsAPY1* and *9* in panicles.

591 The profile of expression from RNA-seq data of *OsAPY*s was investigated to reveal their role
592 in response to different stresses. Their expression profile revealed expression in abiotic and
593 biotic stresses. Figs 12 and 13 show a heat map of their expression profile in biotic and abiotic
594 stress. There was no pre-analyzed RNA-seq data of *OsAPY9*, so the gene expression data of
595 only eight genes were analyzed.

596 **Fig 12. Heatmap of *OsAPY* expression profile in response to various biotic stress**
597 **conditions.** Expression analysis was done utilizing the RNA-seq values of relative expression
598 from GENEVESTIGATOR and using GraphPad Prism 9.0.0, the heat map was generated. The
599 expression profile could be analyzed according to the scale just at the base. The red boxes
600 represent upregulated expression; greens depict downregulated expression, and black boxes
601 signify no change in expression levels.

602 **Fig 13. Heatmap of *OsAPY* expression profile in response to various abiotic stress**
603 **conditions.** Expression analysis was done using the RNA-seq values of relative expression
604 from GENEVESTIGATOR. The heat map was generated using GraphPad Prism 9.0.0. The
605 expression profile could be analyzed according to the scale just at the base. The red boxes

represent upregulated expression; greens depict downregulated expression, and black boxes signify no change in expression levels.

In response to infection by two strains of rice bacterial leaf streak pathogen (*Xanthomonas oryzae* pv. *oryzicola)*, *OsAPY1-5* were upregulated, but *OsAPY8* was downregulated (Fig 12). This finding addressed the role of *OsAPY*s in managing rice stress responses against bacterial leaf streak pathogens. It was observed that the infection with *Rhizoctonia solani* upregulated the expression of *OsAPY2*, *4*, and *8*. Rice blast fungus (*Magnaporthe oryzae*) inoculation induced the expression of *OsAPY2*, *5*, and *8* indicating their possible role in rice blast disease. Infection with rice dwarf virus (RDV) upregulated the expression of *OsAPY1-5*; on the other hand, *OsAPY6*, *8* were downregulated. *OsAPY2*, *3*, *5*, and *8* got upregulated in response to rice stripe virus (RSV) infection, but at the same time, *OsAPY1* and *6* got downregulated.

During anoxic conditions, the expression of *OsAPY1-3* and *8* was upregulated, but *OsAPY4* and *5* were downregulated (Fig 13). *OsAPY4* showed a slight increase in expression only in 3 hours-long anoxic conditions. In *OsAPY8*, the level of expression was proportional to the duration of the anoxic condition. Rice subjected to drought for 2 and 3 days showed upregulation of *OsAPY4* and *5*, but all the other *OsAPY*s, especially *OsAPY7*, were downregulated except *OsAPY6*, which showed no change in expression. The extended period of drought condition downregulated the expression level. The gene expression level increased with time duration in heat stress, but after a specific time, it started to decrease. In the case of heat treatment for 120 minutes, the expression of *OsAPY1-6* was upregulated, but gene expression levels reduced during an extended period of heat treatment (165 minutes). This result indicated that *OsAPY*s displayed late-term responses to heat stress, but extended stress interrupted their expression. When subjected to dehydration, similar late-term expression was observed. 135 minutes long dehydration stress induced the expression of all the *OsAPY*s except *OsAPY4* and *7*. Under salt stress, the expression was relatively higher in leaves than in roots.

All the genes except *OsAPY1*, *5*, and *6* were upregulated in leaves, whereas in root tissues, only *OsAPY5*, *7*, and *8* were upregulated. Under submergence stress, the expression level got increased with the increase in time. As the heatmap depicted (Fig 13), after 22 days of submergence for 24 hours, there was an increase in the expression of *OsAPY1*, *3*, *5*, and *8*. *OsAPY5* and *8* had an increased expression after prolonged exposure to submerged conditions as there was no significant expression in the case of short-term exposure to submerged conditions. Alkali treatment upregulated the expression of *OsAPY5*, *6*, and especially of *8*, whereas for *OsAPY2* and *8*, the expression was induced in cold.

Investigation of expression profile using RT-qPCR data in response to several abiotic stresses

Relative expression ratio of *OsAPY* genes in the rice seedling leaves was assessed under cold, cadmium, salinity, submergence, drought, and heat stress. Heat map of their real-time expression data in these different stress conditions after 18-20 hours is depicted in Fig 14.

Fig 14. Analysis of relative expression of *OsAPY*s under various abiotic stresses. The Y-axis depicts the relative expression of each gene analyzed via RT-qPCR in the rice plant leaves. The X-axis indicates the various abiotic stress conditions under which the relative expression analysis was done. Technical replication was used to find the mean value of expression at different treatments. MS Office 365 and GraphPad Prism 9.0.0 were used to analyze the data. A one-way ANOVA, followed by a Bonferroni post hoc test, was used to assess the significant differences ($P \leq 0.05$). To represent the significant differences, different means were labeled with different number of stars (*).

As shown in Fig 14, all the *OsAPY* genes except *OsAPY8* and *9* showed significantly higher expression under heat stress. Among all the stress environments, *OsAPY5* had considerably

higher expression levels (more than five-fold) in all the stress conditions. The RNA-seq data (Fig 13) also demonstrated its enhanced expression during drought, submergence, dehydration, alkali, salt, and heat stress.

Cold, submergence, drought, and heat stress, all resulted in considerably more significant levels of *OsAPY1* expression. The expression level during submergence stress (more than ten-fold) was significantly higher, and the result obtained from RNA-seq data (Fig 13) corroborated this observation. Under cadmium, cold, salinity, submergence, and heat stress, *OsAPY2* demonstrated significant expression, and RNA-seq data revealed consistent outcomes (Fig 13), especially in cold conditions, its expression was very high. However, the real-time expression level was much more significant in response to cadmium and salinity stress. *OsAPY3* expression was substantially increased in heat and cold stress. Compared to the control condition, it was much greater during cold stress and demonstrated an 8-fold upregulation. Only heat stress raised the expression of *OsAPY4* (approximately eight-fold) and *7* (more than four-fold), whereas salinity and heat stress significantly downregulated the expression of *OsAPY9*. Under heat stress, RNA-seq data also revealed a higher level of *OsAPY4* expression. During cadmium, cold, salinity, and heat stress, *OsAPY6* expression was significantly enhanced, and RNA-seq data also exhibited upregulated expression under salinity and heat stress (Fig 13). Under cadmium, salinity, submergence, drought, and heat stress, *OsAPY8* demonstrated significant downregulation. Though the expression under cold conditions was higher, it was not significant. Its downregulated expression level during drought, heat, and submergence stress and the increased one in cold was also supported by RNA-seq data. According to RNA-seq data, prolonged exposure to submerged situations increased its expression. This result indicates a potential function for *OsAPY*s in regulating abiotic stress.

Discussion

678 A significant role is played by apyrase (*APY*) in regulating the growth of plants, developmental
679 changes, and different stresses [18,24]. When the plants encounter any stress, the extracellular
680 ATP (eATP) level rises which in turn increases ROS expression, triggers several other stress-
681 induced genes, and can also cause apoptosis [5,17]. Apyrase can hydrolyze eATP [134], and
682 thus it has a major function in regulating eATP-mediated ROS production, and cellular
683 apoptosis and in providing tolerance towards various stress conditions. The majority of the
684 world takes rice as their main diet, and Asia alone contributes 90% to global rice production
685 [135]. Different stresses are blamed for yield losses in commercially essential crops in many
686 parts of the world. So, manipulating *APY*s can be a great step towards developing genetically
687 modified multiple stress-tolerant rice and improving its annual production as *APY*s are
688 associated with various developmental stages as well as stress responses of the plants. For this,
689 the *APY* gene family should be studied intensively. Wheat and *Arabidopsis* have been
690 extensively investigated for this gene family [2,23], but an investigation in rice is still not
691 conducted. This study was designed to identify, characterize, and for analyzing the patterns of
692 *APY* expression in rice.

693 Rice was found to have nine apyrase genes, as per this study, and all of these genes contained
694 all the 5 ACRs [22]. An expanded insight into the significance of apyrase under abiotic and
695 biotic stress was gained by the identification, characterization, and profiling of the expression
696 of *APY* genes. These genes are different in their sequence length, molecular weight, pI value,
697 and GRAVY value which means that this gene family is diverse. The GRAVY value of the
698 proteins is negative, confirming the proteins are hydrophilic [92].

699 Ecto-APYs are usually present on plasma membrane and other cell surfaces, and endo-APYs
700 are localized on ER, Golgi body, etc. [23,136], and extracellular ATP is regulated by both endo-
701 and ecto-APYs [19,137]. In this investigation, the proteins were present on the plasma
702 membrane, mitochondria, endoplasmic reticulum, and chloroplast, suggesting that both endo-

703 APYs and ecto-APYs are present in rice [2,23]. Nevertheless, the localization of OsAPY3, 4,
704 and 9 varies according to the two different tools. Findings of CELLO [58] indicated there are
705 three ecto-APYs (OsAPY2, 4, 5), but WoLF PSORT [57] suggested there are two ecto-APYs
706 (OsAPY2, 5). It will take further research to find their precise position.

707 During evolution, gene duplication has a significant contribution in the process of gene
708 expansion., and during plant development and growth, gene duplication can assist plants in
709 adapting to various conditions [138]. The study of duplication events identified six duplication
710 occurrences within the genome. The evolution of these genes occurred under the influence of
711 purifying selection, which was suggested by the value of Ka/Ks, which was less than 1 [93].
712 These duplications occurred in genes situated on different chromosomes, indicating the
713 segmental type of duplication being the main force of diversification [93]. Although segmental
714 duplication preserves the primary functional group, it leads to differentiation in the manner of
715 duplicated genes [139].

716 *OsAPY*s were related to *APY*s from *Arabidopsis* and wheat by constructing a phylogenetic tree
717 in order to better understand their structure and functions. It was found that the phylogenetic
718 tree was composed of three distinct groupings. According to earlier research on *Arabidopsis*
719 and wheat *APY*s, this conclusion is in accordance [2,23]. None of the *OsAPY*s was categorized
720 as members of any new group. *OsAPY* was found to be a very archaic family of genes,
721 originating before even the splitting of monocotyledon (rice and wheat) and dicotyledon
722 (*Arabidopsis*) plants because the *OsAPY* genes shared an equal number of groups with the
723 *AtAPY* genes and with the *TaAPY* genes [140].

724 The number and orientation of exon-introns in plant genes play an essential role in evolution
725 [141]. Gene structure analysis predicted that there was no intronless gene which indicates their
726 high expression, and this gene family is an ancient one and not recently evolved [142,143].

OsAPY5 contained the lowest exon and intron, and *OsAPY6* contained maximum exons and introns. Although *OsAPY1*, *3*, *6* belonged to group I of the phylogenetic tree, their exon-intron structure was different from the other members of group I. *OsAPY2* and *OsAPY4* belonged to group II, but their gene structure was consistent with the other members of group I. *OsAPY5* which belonged to group III had a completely different exon-intron structure.

Conserved motifs are essential for proteins to be functional; and for their specificity. In order to better understand how proteins interact, it is helpful to find the common patterns in structure among them [144]. Conserved motif analysis revealed that motif 1, 5, 8, and 10 were conserved across all OsAPYs; motif 2 was present in all the OsAPYs except OsAPY2. Motif 3, 4, 6, 7, and 9 were the least distributed. These were present only in group I of phylogenetic tree, and the members of each phylogenetic group had an almost similar structure. Their function analysis revealed that 8 of the identified motifs are members of the GDA1-CD39 family, which confirms that the identified genes are members of this GDA1-CD39 nucleosidephosphatase superfamily.

The percentage of alpha-helix, beta-sheet, isolated beta bridge, turn, coil, and 310-helix was similar in all the proteins. The secondary structure analysis showed the dominance of alpha-helix over other structures, which implied the stability of the protein structure [132]. The membrane-spanning motif numbers varied from 0 to 2, which are similar to the previous findings [2,23]. Proteins containing one motif had only N- terminal MSM. The proteins with two motifs had both N- and C- terminal MSMs except OsAPY6, which had only 2 N-terminal MSMs. N- as well as C- terminal MSMs are found in OsAPY2, 4, and 5. These proteins with both the N- and C- terminal MSMs were considered as ecto-APYs according to CELLO [58]. In the earlier studies on human APYs, proteins containing both the MSMs were also predicted to be ecto-APYs [2]. This finding is in accordance with the result obtained from CELLO [58] and TMHMM web servers [78].

The tertiary structure analysis revealed that the predicted structures of all the proteins were of good quality, as confirmed by various tools. These structures could be utilized in analyzing the proteins more precisely in future research. Their docking analysis showed that there existed four categories of bonds between the proteins and their ligand ATP. The high numbers of hydrogen bonds corroborate the stability of the protein-ligand complex, as the stability of such complexes is typically facilitated by these bonds [145].

In the promoter region of a gene, cis-elements and transcription factors (TFs) interact, where they initiate gene transcription by assembling into the transcription initiation complex and then activating the RNA polymerase. [101]. Sixty-nine cis-elements were identified in *OsAPY*s and categorized into eight groups. They were essential in regulating various kinds of stresses and developmental stages, which indicates the engagement of *OsAPY*s in such situations. In plants, the evolution and expression of a character are determined by the gene's chromosomal position. [107]. In this study, genes were unevenly distributed throughout the genome, and chromosomes 3, 7, 8, 10, 11, 12 contained all the *OsAPY* genes, and chromosome 11 contained the maximum number of *OsAPY* genes.

We discovered six distinct hormone-sensitive elements within the promoter region, including abscisic acid, gibberellin, auxin, salicylic acid, ethylene, and methyl-jasmonate responsive cis-elements. The involvement of *APY* in maintaining the level of auxin and ethylene [146] and in controlling the closure of stomata in drought condition induced by abscisic acid [147] was well documented. Moreover, there is ample evidence regarding the crosstalk between ethylene, gibberellin, and auxin [148,149,150]. These previous findings and the present study indicate the probable significance of *OsAPY*s in respective hormonal pathways.

miRNA-mediated regulation of genes has a vital function in controlling the environmental stimuli responsiveness of plants [38]. In this investigation, 103 miRNAs which target the

776 *OsAPY* family members of rice were identified. Twenty-three miRNAs targeted more than one
777 gene, but the rest were specific to only one gene. osa-miR5819 targeted four different genes. It
778 implies that osa-miR5819 could have an important function in the expression of *OsAPY*s.
779 Maximum of the miRNAs were found to be downregulated in many stresses and tissues, with
780 exceptions of osa-miR159a.1, osa-miR5532, osa-miR408-3p and osa-miR3979-3p.
781 Comparatively, the miRNAs showed reduced expression when subjected to various stresses;
782 as plants adapt to growth conditions and environmental stressors, the miRNA-mediated control
783 of *OsAPY* genes could have a decisive role.

784 As per the 3K SNP search database, the prevalence of nonsynonymous SAPs in *OsAPY*s is
785 significantly greater for indica rice cultivars than other rice cultivars. *OsAPY1*, *5*, and *8* showed
786 no SAPs in the studied varieties. Results indicate that the *OsAPY1*, *5*, and *8* are substantially
787 conserved among the studied genotypes. *OsAPY2* contained the maximum number of SAPs
788 which was 5 SAPs. The studied varieties are stress-responsive [38,75] the presence of SAPs
789 indicates their stress responsiveness might be related to these SAPs [151]. For fully
790 comprehending their stress response basis, extensive research is required.

791 The involvement of *OsAPY*s in various tissues during the development and growth of rice was
792 determined by an analysis of their expression patterns (Fig 11) using RNA-seq data. *OsAPY1-*
793 *4*, *9* showed higher levels of gene expression in inflorescence, implying their possible function
794 in flower development. Earlier studies have proven the role of *APY* in flowers [25,152].
795 *OsAPY2* and *4* had an abundant expression in anther, whereas *OsAPY1*, *3-5* showed elevated
796 expression in the pistil, suggesting their potential roles in the germination of pollen,
797 fertilization, and reproduction, respectively. The activity of *APY*s in pollen and pistils was
798 reported in *Arabidopsis* [25,32]. *OsAPY9* expression was found to be higher in the leaves and
799 seedling stage, indicating that it plays a potential function in leaf development and early phases
800 of plant growth. The involvement of *APY*s in leaves has previously been documented in

Medicago truncatula [152] and *Arabidopsis* [25]. Another research on pea seedlings found that *APY*s were involved in early growth and development [153].

To further consider the dynamics of the *OsAPY*s in various biotic and abiotic stresses, their expression profiles via RNA-seq data were studied. The activity of *OsAPY*s was investigated in response to bacteria, fungus, and viruses, and *OsAPY1-5*, and *8* exhibited higher activation. *APY*s have been discovered to function in defensive and symbiotic relationships between plants and microorganisms [154]. *OsAPY1-5* demonstrated higher activity under blight-causing bacteria *Xanthomonas oryzae* pv. *oryzicola*. Both types of viral infections elevated the expression of *OsAPY2, 3* and *5*; under fungal infection, the expression of *OsAPY2*, *5*, and *8* increased. This discovery is in line with an earlier study that found the pea *APY* gene (*PsAPY1*) to be engaged in delivering protection against fungal infections [155]. The analysis of cis-elements showed that in the promoter region of *OsAPY*s, WRE3, WUN motifs, and W-box, that regulate biotic stresses in plants were present. The presence of such motifs corroborates our findings regarding the involvement of these genes in providing a defence under such stress conditions.

To identify the role of *OsAPY*s in abiotic stresses, the data retrieved from the RNA-seq database and the RT-qPCR analysis result were correlated. *OsAPY2* and *8* were essential genes concerning cold stress in both cases, suggesting their potential role under cold condition. In cold condition, *APY* involvement has been reported in *Populus euphratica* (*PeAPY2*) [134]. *OsAPY1*, *2*, and *5* showed increased activity under submergence stress suggesting their probable involvement in this condition. *OsAPY1-6* had upregulated expression under heat stress, suggesting these genes' involvement in heat stress. Under salt stress, *OsAPY2* and *6* demonstrated elevated expression in both cases, indicating their role in helping the plant survive under salt stress. Similar results were found in wheat, where majority of the *APY* genes had higher expression after being exposed to salt for 12 hours in both roots and leaves [23].

826 *OsAPY5* showed higher expression under drought conditions indicating its role in helping
827 plants cope with this condition, as the role of *APY* was previously reported in a study where
828 the pea ectoapyrase was expressed in soybean and *Arabidopsis* and it resulted in better growth
829 and tolerance towards drought conditions [156]. Presence of many abiotic stress responsive
830 cis-elements support the notion concerning the role of *APY*s in abiotic stress conditions. Gene
831 expression is one of the complicated biological processes, and it requires further research for
832 elucidating mechanisms of the *OsAPY*s behind the regulation of several stresses. These findings
833 indicate the function of *OsAPY*s under diverse biotic and abiotic stresses, and so this gene
834 family could prove to be an important candidate for genetic engineering that can provide
835 protection against various stress conditions.

836 Conclusion

837 In this study, the rice *APY* gene family has been identified, characterized, and its expression
838 profiling has been done extensively. Nine genes were identified, and they were found to be
839 located on chromosome 3, 7, 8, 10, 11 and 12. Phylogenetic analysis grouped the nine identified
840 *OsAPY* genes into three groups, and the identified cis-elements revealed their involvement in
841 different stress conditions, hormonal regulation, and developmental stages. This ancient gene
842 family evolved via segmental duplication and some SAPs were present in the stress-responsive
843 varieties, which might contribute to their response to stresses. Four different categories of
844 bonds were identified between the OsAPYs and ATP, suggesting strong docking interactions
845 between them. miRNA analysis helped in understanding the function of miRNA in modulating
846 *OsAPY* activity, while expression profiling via RNA-seq data unveiled the role of *OsAPY*s
847 under various growth phases as well as stresses. The expression analysis using RT-qPCR data
848 also confirmed the response of *OsAPY*s in various abiotic stress conditions, especially in heat
849 stress. These findings would give the insight to broaden the understanding and knowledge

regarding *APY*s in rice as well as provide foundation in future research regarding *OsAPY*s also in the genomic alterations towards the improving of rice and eventually developing stress-tolerant varieties.

Acknowledgements

The authors are thankful to the Plant Genetic Engineering Lab, Department of Genetic Engineering and Biotechnology, Shahjalal University of Science and Technology, Sylhet for supporting to conduct this research.

References

1. Knowles AF. The GDA1_CD39 superfamily: NTPDases with diverse functions. Purinergic Signal. 2011 Mar;7(1):21-45.
2. Chiu TY, Lao J, Manalansan B, Loqué D, Roux SJ, Heazlewood JL. Biochemical characterization of *Arabidopsis* APYRASE family reveals their roles in regulating endomembrane NDP/NMP homoeostasis. Biochem J. 2015 Nov 15;472(1):43-54.
3. Thomas C, Rajagopal A, Windsor B, Dudler R, Lloyd A, Roux SJ. A Role for Ectophosphatase in Xenobiotic Resistance. Plant Cell. 2000 Apr;12(4):519-33.
4. Wu J, Steinebrunner I, Sun Y, Butterfield T, Torres J, Arnold D, et al. Apyrases (Nucleoside Triphosphate-Diphosphohydrolases) Play a Key Role in Growth Control in Arabidopsis. Plant Physiol. 2007 Jun;144(2):961-75.
5. Song CJ, Steinebrunner I, Wang X, Stout SC, Roux SJ. Extracellular ATP Induces the Accumulation of Superoxide via NADPH Oxidases in Arabidopsis. Plant Physiol. 2006 Apr;140(4):1222-32.

6. Kim SY, Sivaguru M, Stacey G. Extracellular ATP in Plants. Visualization, Localization, and Analysis of Physiological Significance in Growth and Signaling. Plant Physiol. 2006 Nov;142(3):984-92.
7. Wu SJ, Liu YS, Wu JY. The Signaling Role of Extracellular ATP and its Dependence on Ca^{2+} Flux in Elicitation of *Salvia miltiorrhiza* Hairy Root Cultures. Plant Cell Physiol. 2008 Apr;49(4):617-24.
8. Chivasa S, Ndimba BK, Simon WJ, Lindsey K, Slabas AR. Extracellular ATP Functions as an Endogenous External Metabolite Regulating Plant Cell Viability. The Plant Cell. 2005 Nov;17(11):3019-34.
9. Jeter CR, Tang W, Henaff E, Butterfield T, Roux SJ. Evidence of a novel cell signaling role for extracellular adenosine triphosphates and diphosphates in Arabidopsis. The Plant Cell. 2004 Oct;16(10):2652-64.
10. Kim SH, Yang SH, Kim TJ, Han JS, Suh JW. Hypertonic Stress Increased Extracellular ATP Levels and the Expression of Stress-Responsive Genes in *Arabidopsis thaliana* Seedlings. Biosci Biotechnol Biochem. 2009 Jun;73(6):1252-6.
11. Weerasinghe RR, Swanson SJ, Okada SF, Garrett MB, Kim SY, Stacey G, et al. Touch induces ATP release in Arabidopsis roots that is modulated by the heterotrimeric G-protein complex. FEBS Lett. 2009 Aug 6;583(15):2521-6.
12. Huang GT, Ma SL, Bai LP, Zhang L, Ma H, Jia P, et al. Signal transduction during cold, salt, and drought stresses in plants. Mol Biol Rep. 2012 Feb;39(2):969-87.
13. Zhu JK. Salt and Drought Stress Signal Transduction in Plants. Annu Rev Plant Biol. 2002;53:247-73.
14. Roux SJ, Steinebrunner I. Extracellular ATP: an unexpected role as a signaler in plants. Trends Plant Sci. 2007 Nov;12(11):522-527.

15. Tang W, Brady SR, Sun Y, Muday GK, Roux SJ. Extracellular ATP Inhibits Root Gravitropism at Concentrations That Inhibit Polar Auxin Transport. Plant Physiol. 2003 Jan;131(1):147-54.

16. Demidchik V, Shang Z, Shin R, Thompson E, Rubio L, Laohavisit A, et al. Plant extracellular ATP signalling by plasma membrane NADPH oxidase and Ca^{2+} channels. Plant J. 2009 Jun;58(6):903-13.

17. Tanaka K, Gilroy S, Jones AM, Stacey G. Extracellular ATP signaling in plants. Trends Cell Biol. 2010 Oct;20(10):601-8.

18. Clark G, Roux SJ. Role of Ca^{2+} in Mediating Plant Responses to Extracellular ATP and ADP. Int J Mol Sci.. 2018 Nov 14;19(11):3590.

19. Lim MH, Wu J, Yao J, Gallardo IF, Dugger JW, Webb LJ, et al. Apyrase Suppression Raises Extracellular ATP Levels and Induces Gene Expression and Cell Wall Changes Characteristic of Stress Responses. Plant Physiol. 2014 Apr;164(4):2054-67.

20. Sun J, Zhang CL, Deng SR, Lu CF, Shen X, Zhou XY, et al. An ATP signalling pathway in plant cells: extracellular ATP triggers programmed cell death in *Populus euphratica*. Plant Cell Environ. 2012 May;35(5):893-916.

21. Clark G, Brown KA, Tripathy MK, Roux SJ. Recent Advances Clarifying the Structure and Function of Plant Apyrases (Nucleoside Triphosphate Diphosphohydrolases). Int J Mol Sci. 2021 Mar 23;22(6):3283.

22. Zimmermann H, Zebisch M, Sträter N. Cellular function and molecular structure of ecto-nucleotidases. Purinergic Signal. 2012 Sep;8(3):437-502.

23. Liu W, Ni J, Shah FA, Ye K, Hu H, Wang Q, et al. Genome-wide identification, characterization and expression pattern analysis of APYRASE family members in response to abiotic and biotic stresses in wheat. PeerJ. 2019 Sep 11;7:e7622.

919 24. Clark GB, Morgan RO, Fernandez MP, Salmi ML, Roux SJ. Breakthroughs spotlighting
920 roles for extracellular nucleotides and apyrases in stress responses and growth and
921 development. Plant Sci. 2014 Aug 1;225:107-16.
922 25. Yang J. Functional analyses of Arabidopsis apyrases 3 through 7. In: Molecular, cell and
923 developmental biology. Doctoral Dissertation. The University of Texas at Austin, Austin,
924 TX. 2011. Available from: https://repositories.lib.utexas.edu/handle/2152/ETD-UT-
925 2011-05-3056.
926 26. Leal DB, Streher CA, Neu TN, Bittencourt FP, Leal CA, da Silva JE, et al.
927 Characterization of NTPDase (NTPDase1; ecto-apyrase; ecto-diphosphohydrolase;
928 CD39; EC 3.6.1.5) activity in human lymphocytes. Biochim Biophys Acta. 2005 Jan
929 18;1721(1-3):9-15.
930 27. Handa M, Guidotti G. Purification and Cloning of a Soluble ATP-Diphosphohydrolase
931 (Apyrase) from Potato Tubers (*Solanum tuberosum*). Biochem Biophys Res Commun.
932 1996 Jan 26;218(3):916-23.
933 28. Riewe D, Grosman L, Fernie AR, Wucke C, Geigenberger P. The Potato-Specific
934 Apyrase Is Apoplastically Localized and Has Influence on Gene Expression, Growth, and
935 Development. Plant Physiol. 2008 Jul;147(3):1092-109.
936 29. Day RB, McAlvin CB, Loh JT, Denny RL, Wood TC, Young ND, et al. Differential
937 Expression of Two Soybean Apyrases, One of Which Is an Early Nodulin. Mol Plant
938 Microbe Interact. 2000 Oct;13(10):1053-70.
939 30. Clark G, Torres J, Finlayson S, Guan X, Handley C, Lee J, et al. Apyrase (Nucleoside
940 Triphosphate-Diphosphohydrolase) and Extracellular Nucleotides Regulate Cotton Fiber
941 Elongation in Cultured Ovules. Plant Physiol. 2010 Feb;152(2):1073-83.
942 31. Steinebrunner I, Wu J, Sun Y, Corbett A, Roux SJ. Disruption of Apyrases Inhibits Pollen
943 Germination in Arabidopsis. Plant Physiol. 2003 Apr;131(4):1638-47.

944 32. Yang J, Wu J, Romanovicz D, Clark G, Roux SJ. Co-regulation of exine wall patterning,
945 pollen fertility and anther dehiscence by Arabidopsis apyrases 6 and 7. Plant Physiol
946 Biochem. 2013 Aug;69:62-73.
947 33. Tan Y, Deng S, Sun Y, Zhao R, Jin X, Shen Z, et al. Functional analysis of *Populus*
948 *euphratica PeAPY1* and *PePY2* in enhancing salt and drought tolerance. Genomics Appl
949 Biol. 2014;33(4):860-8.
950 34. Alam I, Lee DG, Kim KH, Park CH, Sharmin SA, Lee H, et al. Proteome analysis of
951 soybean roots under waterlogging stress at an early vegetative stage. J Biosci. 2010
952 Mar;35(1):49-62.
953 35. Shiraishi T. Suppression of Defense Response Related to Plant Cell Wall. Japan
954 Agricultural Research Quarterly: Jpn. Agric. Res. Q. 2013;47(1):21-7.
955 36. Sivamaruthi BS, Kesika P, Chaiyasut C. Anthocyanins in Thai rice varieties: distribution
956 and pharmacological significance. Int Food Res J. 2018 Sep 1;25(5):2024-32.
957 37. Van Nguyen N, Ferrero A. Meeting the challenges of global rice production. Paddy Water
958 Environ. 2006 Mar;4(1):1-9.
959 38. Yadav SK, Santosh Kumar VV, Verma RK, Yadav P, Saroha A, Wankhede DP, et al.
960 Genome-wide identification and characterization of ABA receptor *PYL* gene family in
961 rice. BMC Genomics. 2020 Sep 30;21(1):676.
962 39. Nuruzzaman M, Manimekalai R, Sharoni AM, Satoh K, Kondoh H, Ooka H, et al.
963 Genome-wide analysis of NAC transcription factor family in rice. Gene. 2010 Oct
964 1;465(1-2):30-44.
965 40. Tian C, Wan P, Sun S, Li J, Chen M. Genome-Wide Analysis of the GRAS Gene Family
966 in Rice and *Arabidopsis*. Plant Mol Biol. 2004 Mar;54(4):519-32.

967 41. Katiyar A, Smita S, Lenka SK, Rajwanshi R, Chinnusamy V, Bansal KC. Genome-wide
968 classification and expression analysis of *MYB* transcription factor families in rice and
969 Arabidopsis. BMC Genom. 2012 Dec;13(1):1-9.
970 42. Ross CA, Liu Y, Shen QJ. The *WRKY* Gene Family in Rice (*Oryza sativa*). J Integr Plant
971 Biol. 2007 Jun;49(6):827-42.
972 43. Zhao L, Hu Y, Chong K, Wang T. *ARAG1*, an ABA-responsive DREB gene, plays a role
973 in seed germination and drought tolerance of rice. Ann Bot. 2010 Mar;105(3):401-9.
974 44. Jung KH, Ko HJ, Nguyen MX, Kim SR, Ronald P, An G. Genome-wide identification
975 and analysis of early heat stress responsive genes in rice. J Plant Biol. 2012
976 Dec;55(6):458-68.
977 45. Shabala S. Regulation of Potassium Transport in Leaves: from Molecular to Tissue Level.
978 Ann Bot. 2003 Nov;92(5):627-34.
979 46. Yamaguchi-Shinozaki K, Shinozaki K. Organization of *cis*-acting regulatory elements in
980 osmotic- and cold-stress-responsive promoters. Trends Plant Sci. 2005 Feb;10(2):88-94.
981 47. Amin US, Biswas S, Elias SM, Razzaque S, Haque T, Malo R, et al. Enhanced Salt
982 Tolerance Conferred by the Complete 2.3 kb cDNA of the Rice Vacuolar Na^+/H^+
983 Antiporter Gene Compared to 1.9 kb Coding Region with 5′ UTR in Transgenic Lines of
984 Rice. Front Plant Sci. 2016 Jan 25;7:14.
985 48. Chen JQ, Meng XP, Zhang Y, Xia M, Wang XP. Over-expression of OsDREB genes lead
986 to enhanced drought tolerance in rice. Biotechnol Lett. 2008 Dec;30(12):2191-8.
987 49. Xu K, Xu X, Fukao T, Canlas P, Maghirang-Rodriguez R, Heuer S, et al. *Sub1A* is an
988 ethylene-response-factor-like gene that confers submergence tolerance to rice. Nature.
989 2006 Aug 10;442(7103):705-8.
990 50. Huala E, Dickerman AW, Garcia-Hernandez M, Weems D, Reiser L, LaFond F, et al.
991 The Arabidopsis Information Resource (TAIR): a comprehensive database and web-

992 based information retrieval, analysis, and visualization system for a model plant. Nucleic
993 Acids Res. 2001 Jan 1;29(1):102-5.
994 51. Goodstein DM, Shu S, Howson R, Neupane R, Hayes RD, Fazo J, et al. Phytozome: a
995 comparative platform for green plant genomics. Nucleic Acids Res. 2012
996 Jan;40(D1):D1178-86.
997 52. Kawahara Y, de la Bastide M, Hamilton JP, Kanamori H, McCombie WR, Ouyang S, et
998 al. Improvement of the *Oryza sativa* Nipponbare reference genome using next generation
999 sequence and optical map data. Rice. 2013 Feb 6;6(1):4.
1000 53. Hunter S, Apweiler R, Attwood TK, Bairoch A, Bateman A, Binns D, et al. InterPro: the
1001 integrative protein signature database. Nucleic Acids Res. 2009 Jan;37(suppl_1):D211-
1002 5.
1003 54. Kumar S, Stecher G, Li M, Knyaz C, Tamura K. MEGA X: Molecular Evolutionary
1004 Genetics Analysis across Computing Platforms. Mol Biol Evol. 2018 Jun 1;35(6):1547-
1005 1549.
1006 55. Nicholas KB. GeneDoc: analysis and visualization of genetic variation. Embnew news.
1007 1997;4:14.
1008 56. Wilkins MR, Gasteiger E, Bairoch A, Sanchez JC, Williams KL, Appel RD, et al. Protein
1009 Identification and Analysis Tools on the ExPASy Server. Methods Mol Biol.
1010 1999;112:531-52.
1011 57. Horton P, Park KJ, Obayashi T, Fujita N, Harada H, Adams-Collier CJ, et al. WoLF
1012 PSORT: protein localization predictor. Nucleic Acids Res. 2007 Jul;35(suppl_2):W585-
1013 7.
1014 58. Yu CS, Chen YC, Lu CH, Hwang JK. Prediction of protein subcellular localization.
1015 Proteins. 2006 Aug 15;64(3):643-51.

1016 59. Bailey TL, Boden M, Buske FA, Frith M, Grant CE, Clementi L, et al. MEME SUITE:
1017 tools for motif discovery and searching. Nucleic Acids Res. 2009 Jul
1018 1;37(suppl_2):W202-8.
1019 60. El-Gebali S, Mistry J, Bateman A, Eddy SR, Luciani A, Potter SC, et al. The Pfam protein
1020 families database in 2019. Nucleic Acids Res. 2019 Jan 8;47(D1):D427-D432.
1021 61. Hu B, Jin J, Guo AY, Zhang H, Luo J, Gao G. GSDS 2.0: an upgraded gene feature
1022 visualization server. Bioinformatics. 2015 Apr 15;31(8):1296-7.
1023 62. Bolser D, Staines DM, Pritchard E, Kersey P. Ensembl Plants: Integrating Tools for
1024 Visualizing, Mining, and Analyzing Plant Genomics Data. Methods Mol Biol.
1025 2016;1374:115-40.
1026 63. Guindon S, Gascuel O. A Simple, Fast, and Accurate Algorithm to Estimate Large
1027 Phylogenies by Maximum Likelihood. Syst Biol. 2003 Oct;52(5):696-704.
1028 64. Letunic I, Bork P. Interactive tree of life (iTOL) v3: an online tool for the display and
1029 annotation of phylogenetic and other trees. Nucleic Acids Res. 2016 Jul 8;44(W1):W242-
1030 5.
1031 65. Lee TH, Tang H, Wang X, Paterson AH. PGDD: a database of gene and genome
1032 duplication in plants. Nucleic Acids Res. 2013 Jan;41(D1):D1152-8.
1033 66. Koch MA, Haubold B, Mitchell-Olds T. Comparative Evolutionary Analysis of Chalcone
1034 Synthase and Alcohol Dehydrogenase Loci in *Arabidopsis*, *Arabis*, and Related Genera
1035 (Brassicaceae). Mol Biol Evol. 2000 Oct;17(10):1483-98.
1036 67. Chen C, Chen H, Zhang Y, Thomas HR, Frank MH, He Y, et al. TBtools: An Integrative
1037 Toolkit Developed for Interactive Analyses of Big Biological Data. Mol Plant. 2020 Aug
1038 3;13(8):1194-202.

1039 68. Lescot M, Déhais P, Thijs G, Marchal K, Moreau Y, Van de Peer Y, et al. PlantCARE, a
1040 database of plant *cis*-acting regulatory elements and a portal to tools for *in silico* analysis
1041 of promoter sequences. Nucleic Acids Res. 2002 Jan 1;30(1):325-7.
1042 69. Voorrips RE. MapChart: Software for the Graphical Presentation of Linkage Maps and
1043 QTLs. J Hered. 2002 Jan-Feb;93(1):77-8.
1044 70. Dai X, Zhao PX. psRNATarget: a plant small RNA target analysis server. Nucleic Acids
1045 Res. 2011 Jul;39(suppl_2):W155-9.
1046 71. Kozomara A, Griffiths-Jones S. miRBase: annotating high confidence microRNAs using
1047 deep sequencing data. Nucleic Acids Res. 2014 Jan;42(D1):D68-73.
1048 72. Shannon P, Markiel A, Ozier O, Baliga NS, Wang JT, Ramage D, et al. Cytoscape: A
1049 Software Environment for Integrated Models of Biomolecular Interaction Networks.
1050 Genome Res. 2003 Nov;13(11):2498-504.
1051 73. Gurjar AK, Panwar AS, Gupta R, Mantri SS. PmiRExAt: plant miRNA expression atlas
1052 database and web applications. Database (Oxford). 2016 Apr 13;2016:baw060.
1053 74. Motulsky HJ. Analyzing data with graphpad prism. GraphPad Software. Inc., San Diego,
1054 CA. 1999.
1055 75. Kaur V, Yadav SK, Wankhede DP, Pulivendula P, Kumar A, Chinnusamy V. Cloning
1056 and characterization of a gene encoding MIZ1, a domain of unknown function protein
1057 and its role in salt and drought stress in rice. Protoplasma. 2020 Mar;257(2):475-487.
1058 76. Mansueto L, Fuentes RR, Borja FN, Detras J, Abriol-Santos JM, Chebotarov D, et al.
1059 Rice SNP-seek database update: new SNPs, indels, and queries. Nucleic Acids Res. 2017
1060 Jan 4;45(D1):D1075-D1081.
1061 77. Heinig M, Frishman D. STRIDE: a web server for secondary structure assignment from
1062 known atomic coordinates of proteins. Nucleic Acids Res. 2004 Jul 1;32(suppl_2):W500-
1063 2.

1064 78. Krogh A, Larsson B, von Heijne G, Sonnhammer EL. Predicting transmembrane protein
1065 topology with a hidden Markov model: application to complete genomes. J Mol Biol.
1066 2001 Jan 19;305(3):567-80.
1067 79. Kim DE, Chivian D, Baker D. Protein structure prediction and analysis using the Robetta
1068 server. Nucleic Acids Res. 2004 Jul 1;32(suppl_2):W526-31..
1069 80. Ko J, Park H, Heo L, Seok C. GalaxyWEB server for protein structure prediction and
1070 refinement. Nucleic Acids Res. 2012 Jul;40(W1):W294-7.
1071 81. Guex N, Peitsch MC. SWISS-MODEL and the Swiss-PdbViewer: An environment for
1072 comparative protein modeling. Electrophoresis. 1997 Dec;18(15):2714-23.
1073 82. Laskowski RA, Rullmannn JA, MacArthur MW, Kaptein R, Thornton JM. AQUA and
1074 PROCHECK-NMR: Programs for checking the quality of protein structures solved by
1075 NMR. J Biomol NMR. 1996 Dec;8(4):477-86.
1076 83. Colovos C, Yeates TO. Verification of protein structures: Patterns of nonbonded atomic
1077 interactions. Protein Sci. 1993 Sep;2(9):1511-9.
1078 84. Wiederstein M, Sippl MJ. ProSA-web: interactive web service for the recognition of
1079 errors in three-dimensional structures of proteins. Nucleic Acids Res. 2007
1080 Jul;35(suppl_2):W407-10.
1081 85. Systemes, D., BIOVIA, discovery studio modeling environment. Release 4.5. Dassault
1082 Systemes: San Diego, CA. 2015.
1083 86. Yan Y, Zhang D, Zhou P, Li B, Huang SY. HDOCK: a web server for protein–protein
1084 and protein–DNA/RNA docking based on a hybrid strategy. Nucleic Acids Res. 2017 Jul
1085 3;45(W1):W365-W373.
1086 87. Laskowski RA. PDBsum: summaries and analyses of PDB structures. Nucleic Acids Res.
1087 2001 Jan 1;29(1):221-2.

88. Hruz T, Laule O, Szabo G, Wessendorp F, Bleuler S, Oertle L, et al. Genevestigator V3: A Reference Expression Database for the Meta-Analysis of Transcriptomes. Adv Bioinformatics. 2008;2008:420747.

89. Untergasser A, Cutcutache I, Koressaar T, Ye J, Faircloth BC, Remm M, et al. Primer3--new capabilities and interfaces. Nucleic Acids Res. 2012 Aug;40(15):e115.

90. Jain M, Nijhawan A, Tyagi AK, Khurana JP. Validation of housekeeping genes as internal control for studying gene expression in rice by quantitative real-time PCR. Biochem Biophys Res Commun. 2006 Jun 30;345(2):646-51.

91. Livak KJ, Schmittgen TD. Analysis of Relative Gene Expression Data Using Real-Time Quantitative PCR and the $2^{-\Delta\Delta CT}$ Method. Methods. 2001 Dec;25(4):402-8.

92. Chang KY, Yang JR. Analysis and Prediction of Highly Effective Antiviral Peptides Based on Random Forests. PLoS One. 2013 Aug 5;8(8):e70166.

93. Liu Z, Liu Y, Coulter JA, Shen B, Li Y, Li C, et al. The WD40 Gene Family in Potato (*Solanum Tuberosum* L.): Genome-Wide Analysis and Identification of Anthocyanin and Drought-Related WD40s. Agronomy. 2020 Mar 15;10(3):401.

94. Hattori T, Totsuka M, Hobo T, Kagaya Y, Yamamoto-Toyoda A. Experimentally determined sequence requirement of ACGT-containing abscisic acid response element. Plant Cell Physiol. 2002 Jan;43(1):136-40.

95. Liu X, Sun Z, Dong W, Wang Z, Zhang L. Expansion and Functional Divergence of the SHORT VEGETATIVE PHASE (SVP) Genes in Eudicots. Genome Biol Evol. 2018 Nov 1;10(11):3026-3037.

96. Gubler F, Jacobsen JV. Gibberellin-responsive elements in the promoter of a barley high-pI alpha-amylase gene. Plant Cell. 1992 Nov;4(11):1435-41.

97. Ogawa M, Hanada A, Yamauchi Y, Kuwahara A, Kamiya Y, Yamaguchi S. Gibberellin biosynthesis and response during Arabidopsis seed germination. Plant Cell. 2003 Jul;15(7):1591-604.

98. Heis MD, Ditmer EM, de Oliveira LA, Frazzon AP, Margis R, Frazzon J. Differential expression of cysteine desulfurases in soybean. BMC Plant Biol. 2011 Nov 18;11:166.

99. Yin J, Li X, Zhan Y, Li Y, Qu Z, Sun L, et al. Cloning and expression of BpMYC4 and BpbHLH9 genes and the role of BpbHLH9 in triterpenoid synthesis in birch. BMC Plant Biol. 2017 Nov 21;17(1):214.

100. Shokri-Gharelo R, Bandehagh A, Mahmoudi B, Moti-Noparvar P. In silico study of cis-acting elements revealing the plastid gene involved in oxidative phosphorylation are responsive to abiotic stresses. Acta Biol. Szeged. 2017 Jan 1;61(2):179-88.

101. Sutoh K, Yamauchi D. Two cis-acting elements necessary and sufficient for gibberellin-upregulated proteinase expression in rice seeds. Plant J. 2003 Jun;34(5):635-45.

102. Kim SR, Kim Y, An G. Identification of methyl jasmonate and salicylic acid response elements from the nopaline synthase (nos) promoter. Plant Physiol. 1993 Sep;103(1):97-103.

103. Gong XX, Yan BY, Tan YR, Gao X, Wang D, Zhang H, et al. Identification of cis-regulatory regions responsible for developmental and hormonal regulation of HbHMGS1 in transgenic *Arabidopsis thaliana*. Biotechnol Lett. 2019 Sep;41(8-9):1077-1091.

104. Li N, Wei S, Chen J, Yang F, Kong L, Chen C, et al. OsASR2 regulates the expression of a defence-related gene, Os2H16, by targeting the GT-1 cis-element. Plant Biotechnol J. 2018 Mar;16(3):771-783.

105. Zuckerman GR, Prakash C, Askin MP, Lewis BS. AGA technical review on the evaluation and management of occult and obscure gastrointestinal bleeding. Gastroenterology. 2000 Jan;118(1):201-21.

106. Arefin S, Bhuiyan MF, Akther J, Prodhan SH, Hoque H. The dynamics of cis-regulatory elements in promoter regions of tomato sucrose transporter genes. Int J Veg Sci. 2021 Mar 4;27(2):167-86.

107. Piechulla B, Merforth N, Rudolph B. Identification of tomato Lhc promoter regions necessary for circadian expression. Plant Mol Biol. 1998 Nov 1;38(4):655-62.

108. Ezcurra I, Ellerström M, Wycliffe P, Stålberg K, Rask L. Interaction between composite elements in the napA promoter: both the B-box ABA-responsive complex and the RY/G complex are necessary for seed-specific expression. Plant Mol Biol. 1999 Jul;40(4):699-709.

109. Jin XQ, Chen ZW, Tan RH, Zhao SJ, Hu ZB. Isolation and functional analysis of 4-coumarate: coenzyme A ligase gene promoters from *Salvia miltiorrhiza*. Biol Plant. 2012 Jun;56(2):261-8.

110. Wang X, Zhang H, Shao LY, Yan X, Peng H, Ouyang JX, et al. Expression and function analysis of a rice OsHSP40 gene under salt stress. Genes Genomics. 2019 Feb;41(2):175-182.

111. Hou F, Du T, Qin Z, Xu T, Li A, Dong S, et al. Genome-wide in silico identification and expression analysis of beta-galactosidase family members in sweetpotato [*Ipomoea batatas* (L.) Lam]. BMC Genom. 2021 Dec;22(1):1-3.

112. Kaur A, Pati PK, Pati AM, Nagpal AK. In-silico analysis of cis-acting regulatory elements of pathogenesis-related proteins of *Arabidopsis thaliana* and *Oryza sativa*. PLoS One. 2017 Sep 14;12(9):e0184523.

113. Lois R, Dietrich A, Hahlbrock K, Schulz W. A phenylalanine ammonia-lyase gene from parsley: structure, regulation and identification of elicitor and light responsive cis-acting elements. EMBO J. 1989 Jun;8(6):1641-8.

114. López-Ochoa L, Acevedo-Hernández G, Martínez-Hernández A, Argüello-Astorga G, Herrera-Estrella L. Structural relationships between diverse cis-acting elements are critical for the functional properties of a rbcS minimal light regulatory unit. J Exp Bot. 2007;58(15-16):4397-406.

115. Liu L, Zhang X, Chen F, Mahi AA, Wu X, Chen Q, et al. Analysis of promoter activity reveals that *GmFTL2* expression differs from that of the known *Flowering Locus T* genes in soybean. Crop J. 2017 Oct 1;5(5):438-48.

116. Le Gourrierec J, Li YF, Zhou DX. Transcriptional activation by Arabidopsis GT-1 may be through interaction with TFIIA-TBP-TATA complex. Plant J. 1999 Jun;18(6):663-8.

117. De Silva WS, Perera MM, Perera KL, Wickramasuriya AM, Jayasekera GA. In silico analysis of osr40c1 promoter sequence isolated from Indica variety Pokkali. Rice Sci. 2017 Jul 1;24(4):228-34.

118. Hiratsuka K, Chua NH. Light regulated transcription in higher plants. J Plant Res. 1997 Mar;110(1):131-9.

119. Prabu G, Prasad DT. Functional characterization of sugarcane MYB transcription factor gene promoter (PScMYBAS1) in response to abiotic stresses and hormones. Plant Cell Rep. 2012 Apr;31(4):661-9.

120. Hazra A, Dasgupta N, Sengupta C, Das S. MIPS: Functional dynamics in evolutionary pathways of plant kingdom. Genomics. 2019 Dec;111(6):1929-1945.

121. Haralampidis K, Milioni D, Rigas S, Hatzopoulos P. Combinatorial interaction of cis elements specifies the expression of the Arabidopsis AtHsp90-1 gene. Plant Physiol. 2002 Jul;129(3):1138-49.

122. Wu A, Hao P, Wei H, Sun H, Cheng S, Chen P, et al. Genome-Wide Identification and Characterization of Glycosyltransferase Family 47 in Cotton. Front Genet. 2019 Sep 11;10:824.

123. Chen W, Provart NJ, Glazebrook J, Katagiri F, Chang HS, Eulgem T, et al. Expression profile matrix of Arabidopsis transcription factor genes suggests their putative functions in response to environmental stresses. Plant Cell. 2002 Mar;14(3):559-74.

124. Liu J, Wang F, Yu G, Zhang X, Jia C, Qin J, et al. Functional Analysis of the Maize C-Repeat/DRE Motif-Binding Transcription Factor CBF3 Promoter in Response to Abiotic Stress. Int J Mol Sci. 2015 May 28;16(6):12131-46.

125. Dubouzet JG, Sakuma Y, Ito Y, Kasuga M, Dubouzet EG, Miura S, Seki M, Shinozaki K, Yamaguchi-Shinozaki K. OsDREB genes in rice, *Oryza sativa* L., encode transcription activators that function in drought-, high-salt- and cold-responsive gene expression. Plant J. 2003 Feb;33(4):751-63.

126. Abe H, Urao T, Ito T, Seki M, Shinozaki K, Yamaguchi-Shinozaki K. Arabidopsis AtMYC2 (bHLH) and AtMYB2 (MYB) function as transcriptional activators in abscisic acid signaling. Plant Cell. 2003 Jan;15(1):63-78.

127. Li Z, Li G, Cai M, Priyadarshani SVGN, Aslam M, Zhou Q, et al. Genome-Wide Analysis of the YABBY Transcription Factor Family in Pineapple and Functional Identification of *AcYABBY4* Involvement in Salt Stress. Int J Mol Sci. 2019 Nov 22;20(23):5863.

128. Shinozaki K, Yamaguchi-Shinozaki K. Gene Expression and Signal Transduction in Water-Stress Response. Plant Physiol. 1997 Oct;115(2):327-334.

129. Pandey S, Subramanaym Reddy C, Yaqoob U, Negi Y, Arora S. Insilico analysis of cis acting regulatory elements CAREs in upstream regions of ascorbate glutathione pathway genes from *Oryza sativa*. Biochem Physiol. 2015;4(2).

130. Jiu S, Haider MS, Kurjogi MM, Zhang K, Zhu X, Fang J. Genome-wide Characterization and Expression Analysis of Sugar Transporter Family Genes in Woodland Strawberry. Plant Genome. 2018 Nov;11(3).

131. Tarasov KV, Tarasova YS, Tam WL, Riordon DR, Elliott ST, Kania G, et al. B-MYB is essential for normal cell cycle progression and chromosomal stability of embryonic stem cells. PLoS One. 2008 Jun 25;3(6):e2478.

132. Islam R, Rahaman M, Hoque H, Hasan N, Prodhan SH, Ruhama A, et al. Computational and structural based approach to identify malignant nonsynonymous single nucleotide polymorphisms associated with CDK4 gene. PLoS One. 2021 Nov 4;16(11):e0259691.

133. Muthukumaran J, Manivel P, Kannan M, Jeyakanthan J, Krishna R. A framework for classification of antifreeze proteins in over wintering plants based on their sequence and structural features. J. Bioinform. Seq. Anal. 2011 May;3:70-88.

134. Deng S, Sun J, Zhao R, Ding M, Zhang Y, Sun Y, et al. Populus euphratica APYRASE2 Enhances Cold Tolerance by Modulating Vesicular Trafficking and Extracellular ATP in Arabidopsis Plants. Plant Physiol. 2015 Sep;169(1):530-48.

135. Schneider P, Asch F. Rice production and food security in Asian Mega deltas—A review on characteristics, vulnerabilities and agricultural adaptation options to cope with climate change. J Agron Crop Sci. 2020 Aug;206(4):491-503.

136. Govindarajulu M, Kim SY, Libault M, Berg RH, Tanaka K, Stacey G, et al. GS52 Ecto-Apyrase Plays a Critical Role during Soybean Nodulation. Plant Physiol. 2009 Feb;149(2):994-1004.

137. Pietrowska-Borek M, Dobrogojski J, Sobieszczuk-Nowicka E, Borek S. New Insight into Plant Signaling: Extracellular ATP and Uncommon Nucleotides. Cells. 2020 Feb 2;9(2):345.

1232 138. Huang Z, Duan W, Song X, Tang J, Wu P, Zhang B, et al. Retention, Molecular
1233 Evolution, and Expression Divergence of the Auxin/Indole Acetic Acid and Auxin
1234 Response Factor Gene Families in Brassica Rapa Shed Light on Their Evolution Patterns
1235 in Plants. Genome Biol Evol. 2016 Feb 1;8(2):302-16.
1236 139. Wang Q, Xu X, Cao X, Hu T, Xia D, Zhu J, et al. Identification, Classification, and
1237 Expression Analysis of the Triacylglycerol Lipase (TGL) Gene Family Related to Abiotic
1238 Stresses in Tomato. Int J Mol Sci. 2021 Jan 30;22(3):1387.
1239 140. Liu Q, Sun C, Han J, Li L, Wang K, Wang Y, et al. Identification, characterization
1240 and functional differentiation of the NAC gene family and its roles in response to cold
1241 stress in ginseng, Panax ginseng C.A. Meyer. PLoS One. 2020 Jun 11;15(6):e0234423.
1242 141. Koralewski TE, Krutovsky KV. Evolution of Exon-Intron Structure and Alternative
1243 Splicing. PLoS One. 2011 Mar 25;6(3):e18055.
1244 142. Deshmukh RK, Sonah H, Singh NK. Intron gain, a dominant evolutionary process
1245 supporting high levels of gene expression in rice. J Plant Biochem Biotechnol. 2016
1246 Apr;25(2):142-6.
1247 143. Nagar P, Kumar A, Jain M, Kumari S, Mustafiz A. Genome-wide analysis and
1248 transcript profiling of PSKR gene family members in *Oryza sativa*. PLoS One. 2020 Jul
1249 23;15(7):e0236349.
1250 144. MacIsaac KD, Fraenkel E. Practical Strategies for Discovering Regulatory DNA
1251 Sequence Motifs. PLoS Comput Biol. 2006 Apr;2(4):e36.
1252 145. Elengoe A, Naser MA, Hamdan S. Modeling and Docking Studies on Novel Mutants
1253 (K71L and T204V) of the ATPase Domain of Human Heat Shock 70 kDa Protein 1. Int
1254 J Mol Sci. 2014 Apr 22;15(4):6797-814.
1255 146. Liu X, Wu J, Clark G, Lundy S, Lim M, Arnold D, et al. Role for Apyrases in Polar
1256 Auxin Transport in Arabidopsis. Plant Physiol. 2012 Dec;160(4):1985-95.

147. Zhang Y, Sun Y, Liu X, Deng J, Yao J, Zhang Y, et al. Populus euphratica Apyrases Increase Drought Tolerance by Modulating Stomatal Aperture in Arabidopsis. Int J Mol Sci. 2021 Sep 13;22(18):9892.

148. Smalle J, Haegman M, Kurepa J, Van Montagu M, Straeten DV. Ethylene can stimulate Arabidopsis hypocotyl elongation in the light. Proc Natl Acad Sci U S A. 1997 Mar 18;94(6):2756-61.

149. Saibo NJ, Vriezen WH, Beemster GT, Van Der Straeten D. Growth and stomata development of Arabidopsis hypocotyls are controlled by gibberellins and modulated by ethylene and auxins. Plant J. 2003 Mar;33(6):989-1000.

150. Vandenbussche F, Smalle J, Le J, Saibo NJ, De Paepe A, Chaerle L, et al. The Arabidopsis Mutant alh1 Illustrates a Cross Talk between Ethylene and Auxin. Plant Physiol. 2003 Mar;131(3):1228-38.

151. Morgil H, Gercek YC, Tulum I. Single nucleotide polymorphisms (SNPs) in plant genetics and breeding. The Recent Topics in Genetic Polymorphisms: IntechOpen; 2020.

152. Navarro-Gochicoa MT, Camut S, Niebel A, Cullimore JV. Expression of the Apyrase-Like APY1 Genes in Roots of Medicago truncatula Is Induced Rapidly and Transiently by Stress and Not by Sinorhizobium meliloti or Nod Factors. Plant Physiol. 2003 Mar;131(3):1124-36.

153. Yoneda M, Davies E, Morita EH, Abe S. Immunohistochemical localization of apyrase during initial differentiation and germination of pea seeds. Planta. 2009 Dec;231(1):47-56.

154. Tanaka K, Tóth K, Stacey G. Role of ectoapyrases in nodulation. Biological Nitrogen Fixation. 2015 Aug 3:517-24.

155. Toyoda K, Yasunaga E, Niwa M, Ohwatari Y, Nakashima A, Inagaki Y, et al. H2O2 production by copper amine oxidase, a component of the ecto-apyrase (ATPase)-

containing protein complex(es) in the pea cell wall, is regulated by an elicitor and a suppressor from Mycosphaerella pinodes. J Gen Plant Pathol. 2012 Sep;78(5):311-5.

156. Veerappa R, Slocum RD, Siegenthaler A, Wang J, Clark G, Roux SJ. Ectopic expression of a pea apyrase enhances root system architecture and drought survival in Arabidopsis and soybean. Plant Cell Environ. 2019 Jan;42(1):337-353.

Supporting information

S1 Fig. Apyrase Conserved Region (ACR) analysis of the OsAPYs. The alignment was done using MEGA X and visualized via GeneDoc. The navy blue, pink, and aqua colors indicate the amino acids that are conserved 100%, 80%, and 60%, respectively, and the red-colored boxes depict the apyrase conserved region (ACR).

S2 Fig. Ramachandran plot of the tertiary structures of OsAPYs. The Ramachandran plot was generated via PROCHECK. Residues in the most favored, additional allowed, generously allowed, and disallowed regions are specified via red, yellow, pale yellow, and white colors, respectively.

S3 Fig. ERRAT plot of the tertiary structures of OsAPYs. ERRAT plot was generated via ERRAT. Yellow bars indicate the segment of the proteins which could be excluded at a 95% confidence level, and the red bars denote the ones at a 99% confidence level. The section with a lower error rate is marked by white bars.

S4 Fig. Z-score plot of the tertiary structures of OsAPYs. The Z-score plot was generated via ProSA-web. The light blue color indicates the Z-score of the proteins measured by X-ray crystallography, and the dark blue color indicates the Z-score of the proteins measured by nuclear magnetic resonance (NMR) spectroscopy. Black dots indicate the Z-score of each protein.

S5 Fig. Energy plot of the tertiary structures of OsAPYs. The energy plot was generated via ProSA-web. The dark green line represents the energy averaged across each fragment of 40 residues, and the light green line depicts the one across each fragment of 10 residues.

S6 Fig. Ramachandran plot of the protein (OsAPYs)- ligand (ATP) complex structure. The Ramachandran plot was generated via PROCHECK. Residues in the most favored, additional allowed, generously allowed, and disallowed regions are specified via red, yellow, pale yellow, and white colors, respectively.

S7 Fig. ERRAT plot of the protein (OsAPYs)- ligand (ATP) complex structure. ERRAT plot was generated via ERRAT. Yellow bars indicate the segment of the proteins which could be excluded at a 95% confidence level, and the red bars denote the ones at a 99% confidence level. The section with a lower error rate is marked by white bars.

S1 Table. Description of the conserved motifs in OsAPYs.

S2 Table. Duplicated *APY* genes and the probable dates of duplication blocks in rice.

S3 Table. The location of all the *OsAPY*s in different chromosome, their position, and orientation.

S4 Table. List of miRNAs targeting different *OsAPY*s and their mode of inhibition.

S5 Table. The percentage of alpha-helix, beta-sheet, beta bridge, turn, coil, 310 helix, and the position of the transmembrane motif in the OsAPY members.

S6 Table. Validation score of OsAPY tertiary structure via different tools.

S7 Table. Docking score of the docked complexes generated via HDOCK server.

S8 Table: Number of bonds formed between OsAPYs and ATP according to PDBSum analysis.

1327 **S9 Table. Analysis of the interaction of OsAPY proteins with their ligand (ATP).**

1328 **S10 Table. List of primers used in RT-qPCR analysis.**

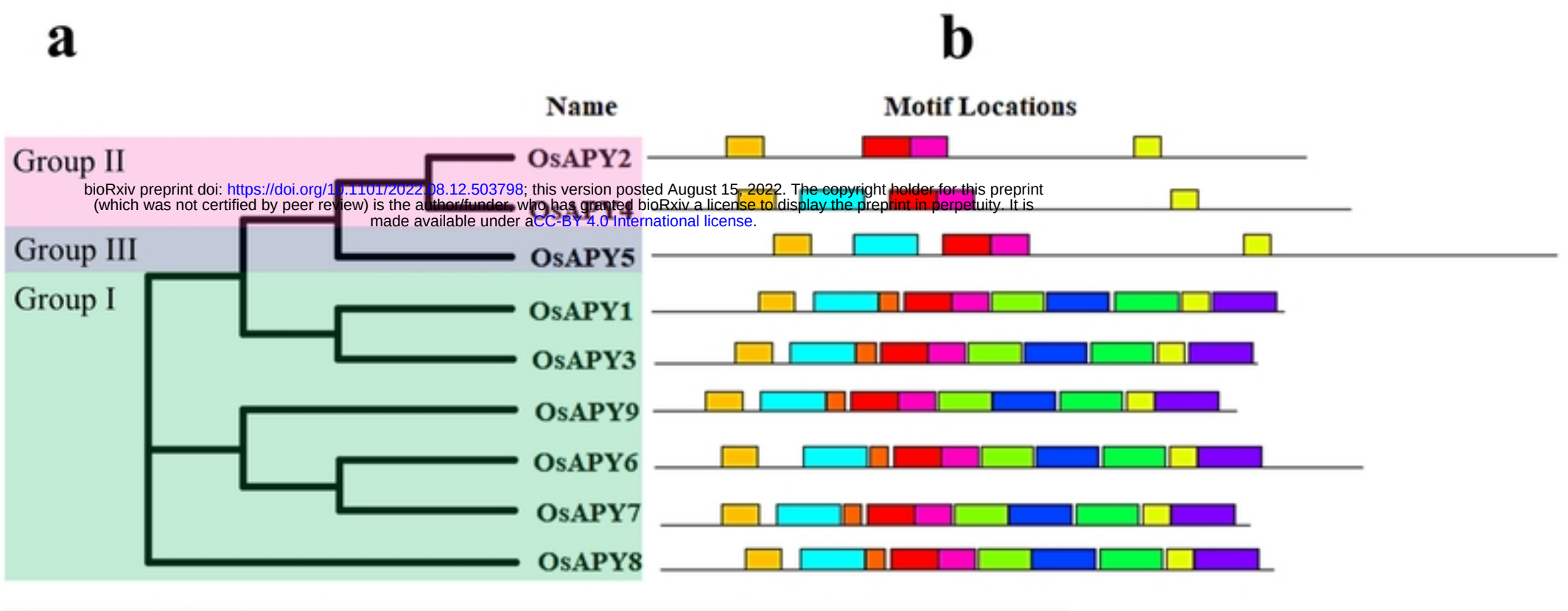

Motif	Symbol	Motif Consensus
1.		FQYQPDWITVLSGSQEGSYAWVALNYLLGKLGGDYSK
2.		PGLSSYAGRPQEAAKSJVPLLEKAKKVVPVELMKKTPLKLGATAGLRLJG
3.		GEDPYVTKEYLKGKDYNJYVHSYLHYGLLASRVEILKRKNG
4.		YLCMDLVYQYTLLVDGFGLEPTKEITLVEKVKHGEYYIEAAWPLGTAIEA
5.		GPGRYAVILDAGSTGSRVHVFRFDKNLDL
6.		CSFNGVWNGGGGAGQDDLYVASYFYDRASEAGFIBSEAPSAKSTPAAFK
7.		FSNCMLRGFSGKYKYNGEQYDASAAPQGADYHKCREDVVKALKLDAPCE
8.		TVGVIDLGGGSVQMAYAISEKLAAEAPKV
9.		EKAEQILEAVRDLVH
10.		EKVCKLSVKEAKAAYPNVSDH

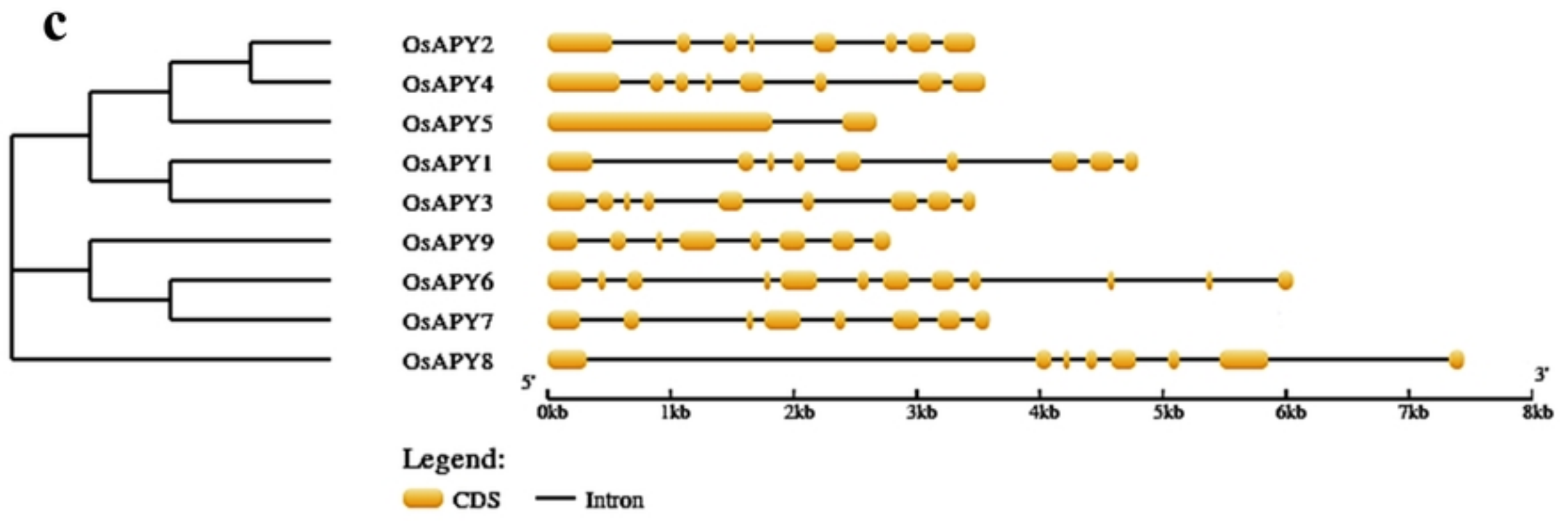

Figure

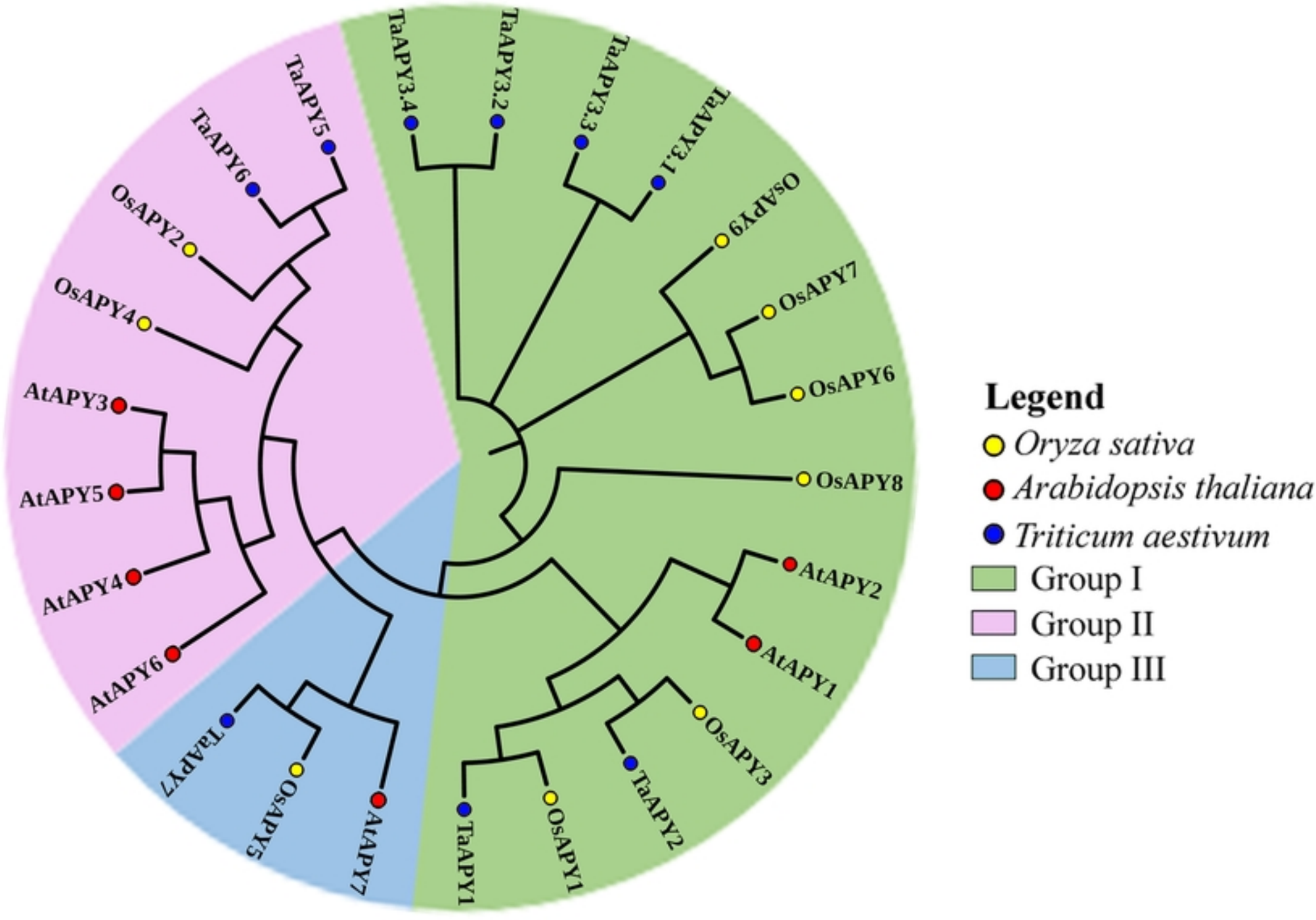
TaAPY3.4
TaAPY3.2
TaAPY3.3
TaAPY3.1
OsAPY9
OsAPY7
OsAPY6
OsAPY8
AtAPY2
AtAPY1
OsAPY3
TaAPY2
OsAPY1
TaAPY1
AtAPY7
OsAPY5
TaAPY7
AtAPY6
AtAPY4
AtAPY5
AtAPY3
OsAPY4
OsAPY2
TaAPY6
TaAPY5
Legend
Oryza sativa
Arabidopsis thaliana
Triticum aestivum
Group I
Group II
Group III

Figure

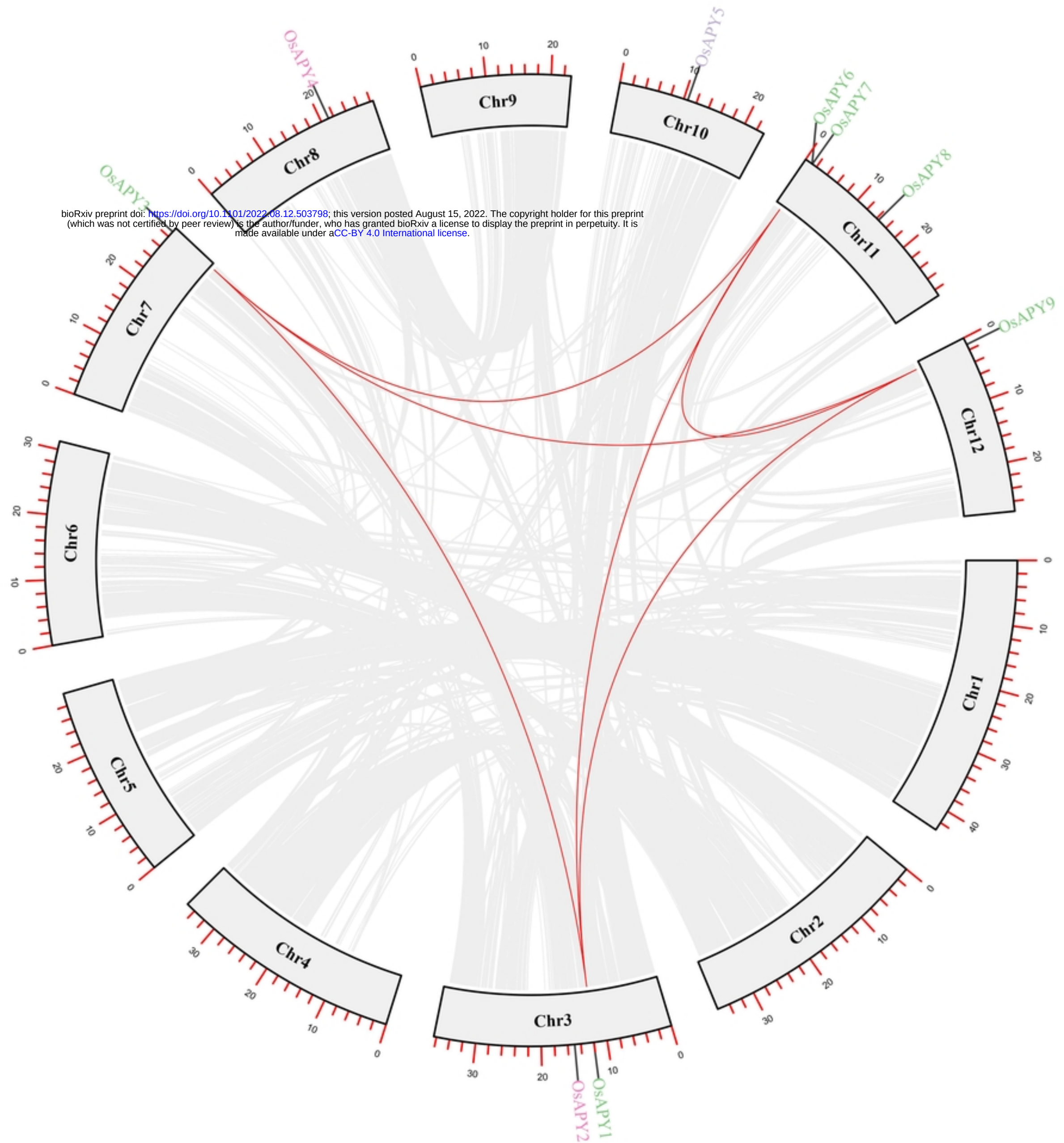

Figure

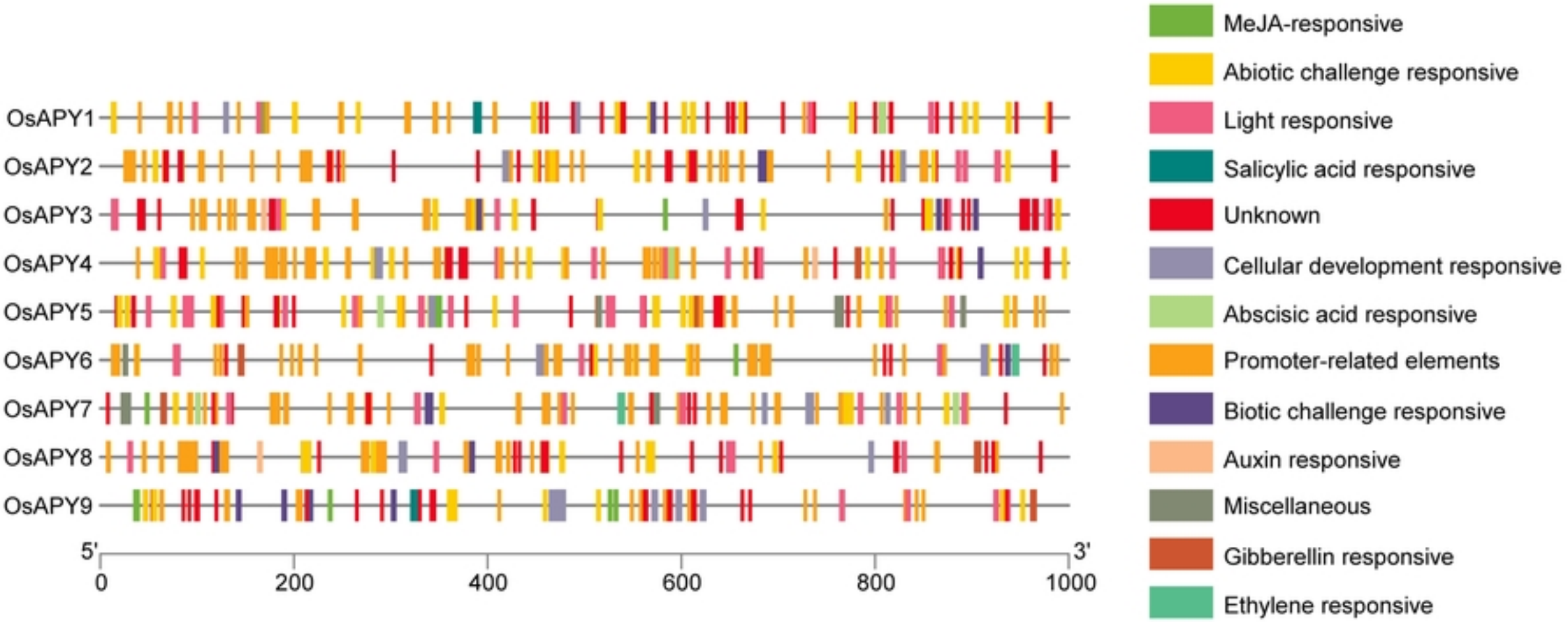
OsAPY1
OsAPY2
OsAPY3
OsAPY4
OsAPY5
OsAPY6
OsAPY7
OsAPY8
OsAPY9
5'
3'
0
200
400
600
800
1000
MeJA-responsive
Abiotic challenge responsive
Light responsive
Salicylic acid responsive
Unknown
Cellular development responsive
Abscisic acid responsive
Promoter-related elements
Biotic challenge responsive
Auxin responsive
Miscellaneous
Gibberellin responsive
Ethylene responsive

Figure

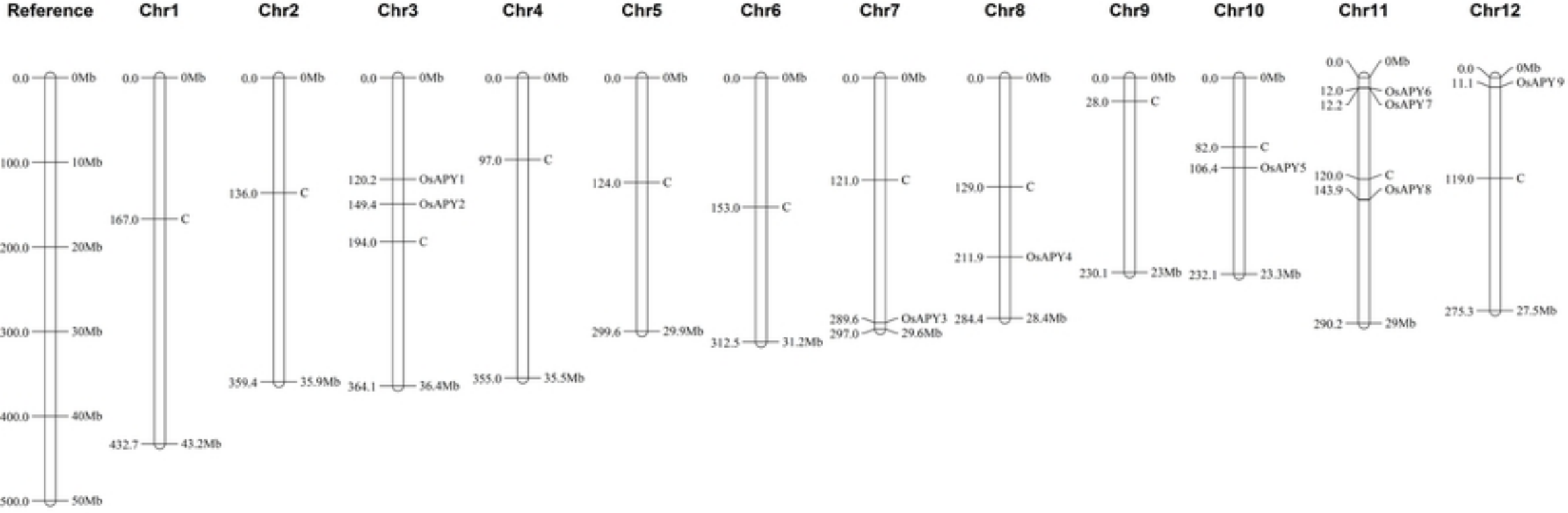
Reference
Chr1
Chr2
Chr3
Chr4
Chr5
Chr6
Chr7
Chr8
Chr9
Chr10
Chr11
Chr12
0.0 0Mb
100.0 10Mb
200.0 20Mb
300.0 30Mb
400.0 40Mb
500.0 50Mb
0.0 0Mb
167.0 C
432.7 43.2Mb
0.0 0Mb
136.0 C
359.4 35.9Mb
0.0 0Mb
120.2 OsAPY1
149.4 OsAPY2
194.0 C
364.1 36.4Mb
0.0 0Mb
97.0 C
355.0 35.5Mb
0.0 0Mb
124.0 C
299.6 29.9Mb
0.0 0Mb
153.0 C
312.5 31.2Mb
0.0 0Mb
121.0 C
289.6 OsAPY3
297.0 29.6Mb
0.0 0Mb
129.0 C
211.9 OsAPY4
284.4 28.4Mb
0.0 0Mb
28.0 C
230.1 23Mb
0.0 0Mb
82.0 C
106.4 OsAPY5
232.1 23.3Mb
0.0 0Mb
12.0 OsAPY6
12.2 OsAPY7
120.0 C
143.9 OsAPY8
290.2 29Mb
0.0 0Mb
11.1 OsAPY9
119.0 C
275.3 27.5Mb

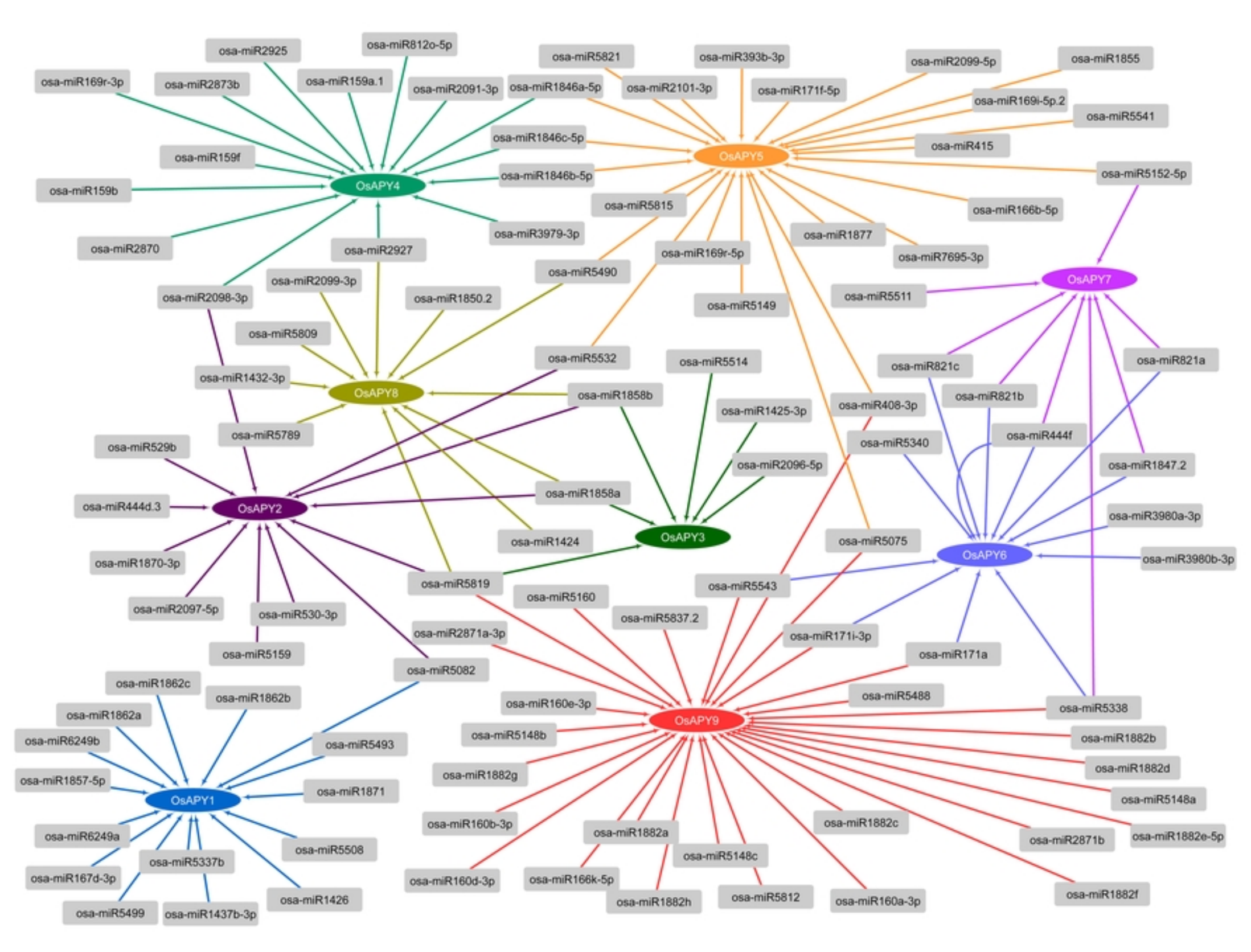
osa-miR2925
osa-miR812o-5p
osa-miR5821
osa-miR393b-3p
osa-miR2099-5p
osa-miR1855
osa-miR169r-3p
osa-miR2873b
osa-miR159a.1
osa-miR2091-3p
osa-miR1846a-5p
osa-miR2101-3p
osa-miR171f-5p
osa-miR169i-5p.2
osa-miR5541
osa-miR1846c-5p
osa-miR415
osa-miR159f
OsAPY5
osa-miR1846b-5p
osa-miR5152-5p
osa-miR159b
OsAPY4
osa-miR5815
osa-miR166b-5p
osa-miR3979-3p
osa-miR1877
osa-miR2870
osa-miR2927
osa-miR169r-5p
osa-miR7695-3p
osa-miR5490
OsAPY7
osa-miR2098-3p
osa-miR2099-3p
osa-miR1850.2
osa-miR5511
osa-miR5149
osa-miR5809
osa-miR5532
osa-miR5514
osa-miR821a
osa-miR821c
osa-miR1432-3p
OsAPY8
osa-miR821b
osa-miR1858b
osa-miR408-3p
osa-miR1425-3p
osa-miR5789
osa-miR444f
osa-miR5340
osa-miR529b
osa-miR1847.2
osa-miR2096-5p
osa-miR444d.3
OsAPY2
osa-miR1858a
osa-miR3980a-3p
OsAPY3
osa-miR1424
osa-miR5075
OsAPY6
osa-miR3980b-3p
osa-miR1870-3p
osa-miR5819
osa-miR5543
osa-miR5160
osa-miR2097-5p
osa-miR530-3p
osa-miR5837.2
osa-miR171i-3p
osa-miR2871a-3p
osa-miR171a
osa-miR5159
osa-miR5082
osa-miR1862c
osa-miR5488
osa-miR160e-3p
osa-miR1862b
osa-miR5338
osa-miR1862a
OsAPY9
osa-miR5148b
osa-miR1882b
osa-miR6249b
osa-miR5493
osa-miR1882g
osa-miR1882d
osa-miR1857-5p
osa-miR1871
OsAPY1
osa-miR5148a
osa-miR160b-3p
osa-miR1882c
osa-miR1882e-5p
osa-miR6249a
osa-miR1882a
osa-miR2871b
osa-miR5508
osa-miR5148c
osa-miR5337b
osa-miR160d-3p
osa-miR166k-5p
osa-miR1882f
osa-miR167d-3p
osa-miR1882h
osa-miR5812
osa-miR160a-3p
osa-miR1426
osa-miR5499
osa-miR1437b-3p

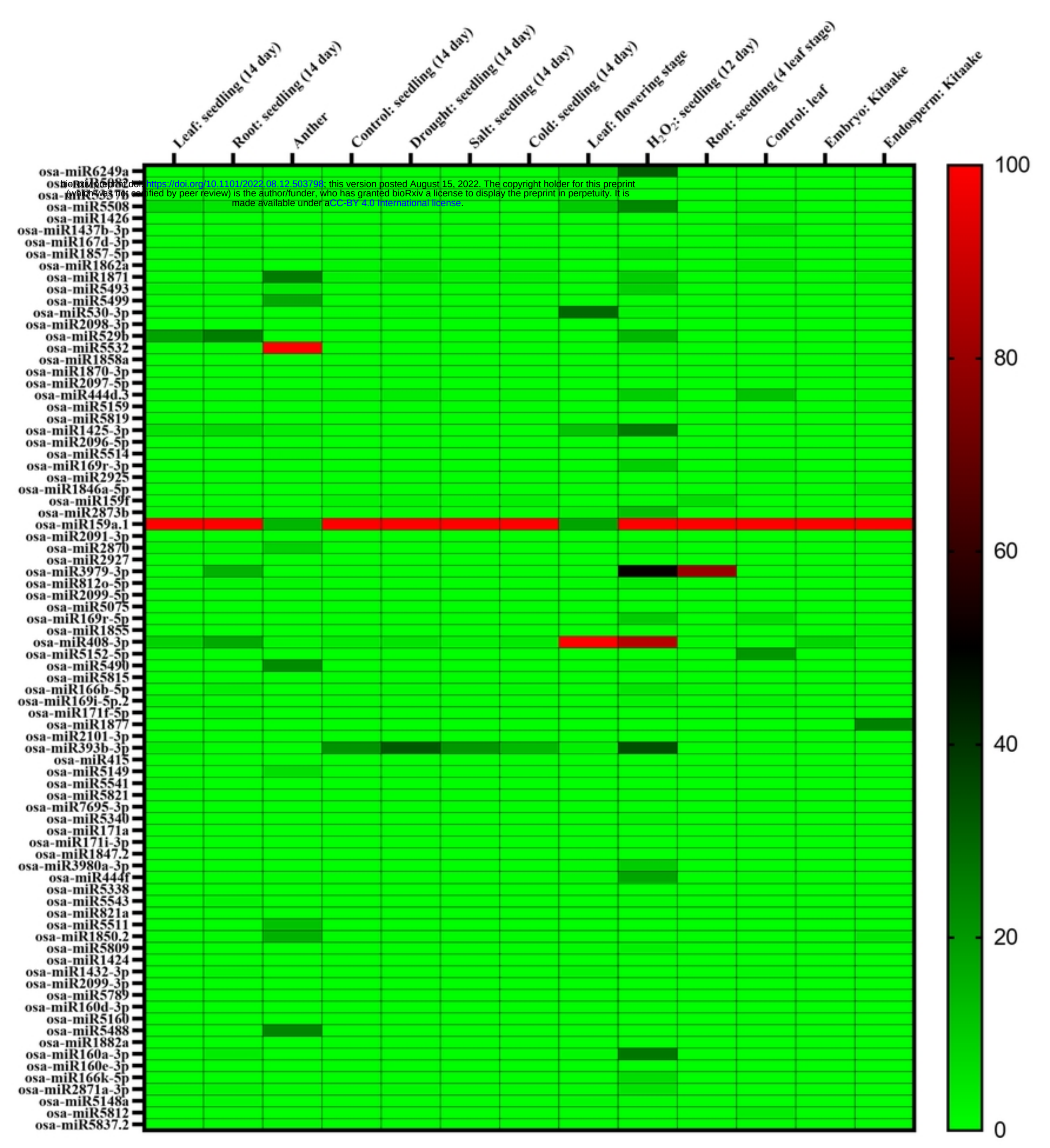

OsAPY1

OsAPY2

OsAPY3

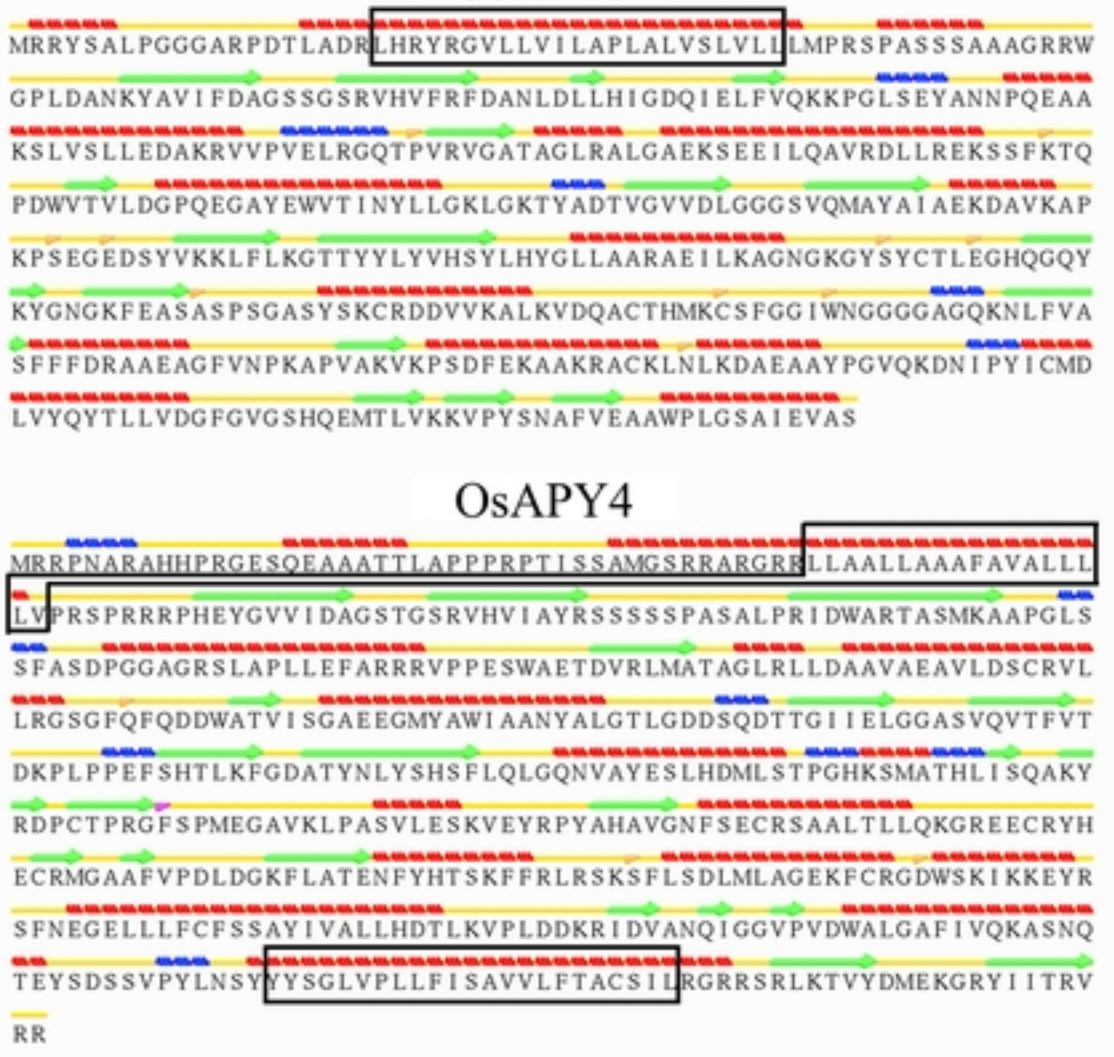

OsAPY4

OsAPY5

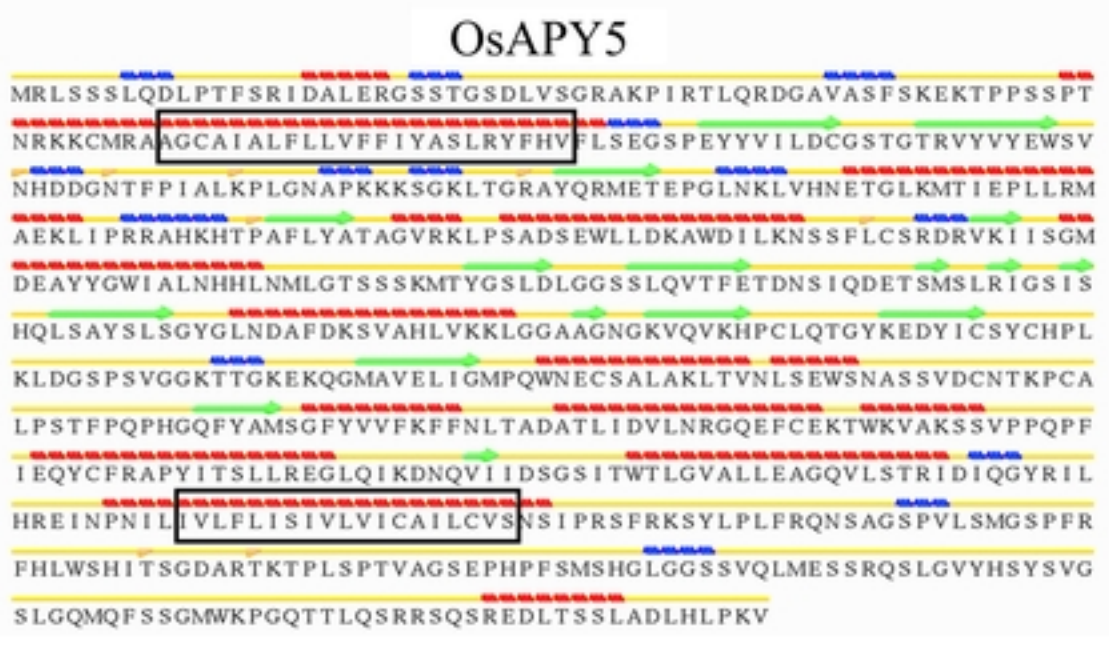

OsAPY6

OsAPY7

OsAPY8

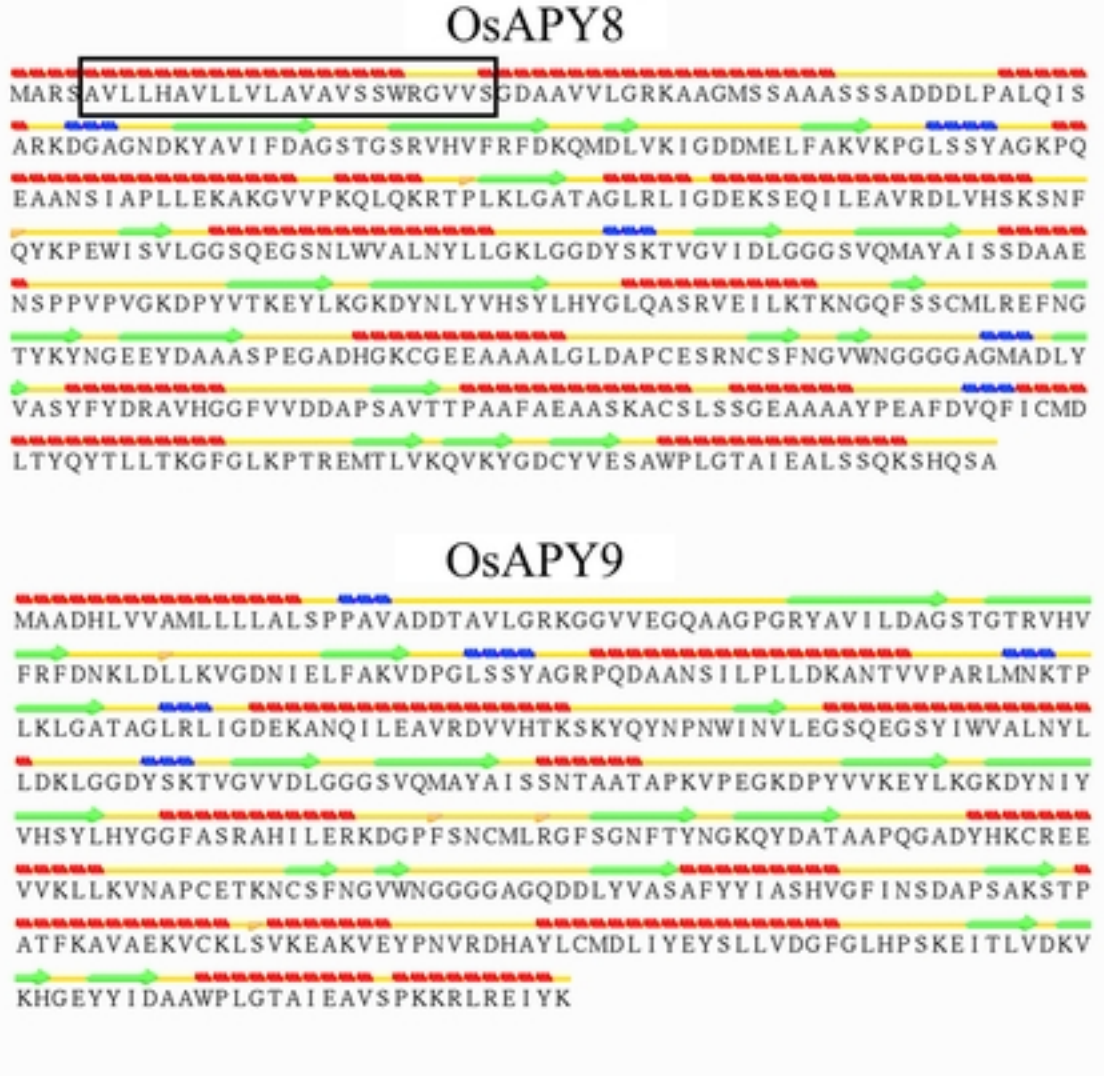

OsAPY9

Legend of secondary structure icons:

H	Alpha-Helix	T	Turn
E	Extended Configuration (Beta-sheet)	C or " "	Coil
B	Isolated Beta Bridge	G	3-10 Helix
b	Isolated Beta Bridge (Type 3 Fig 4,cd)	I	Pi-Helix

OsAPY1

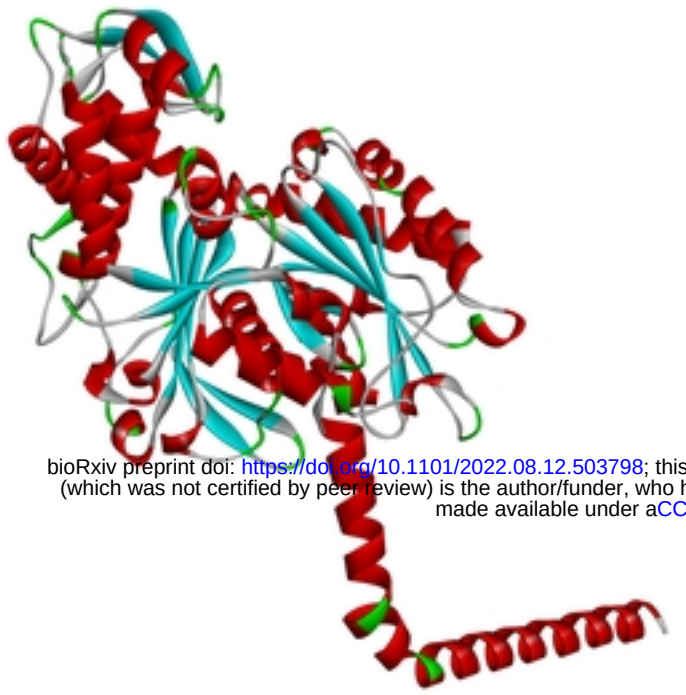

OsAPY2

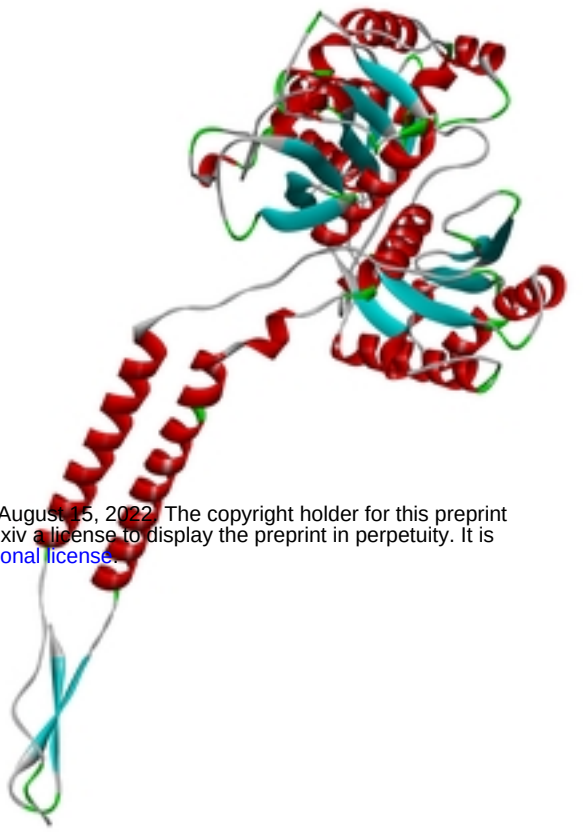

OsAPY3

OsAPY4

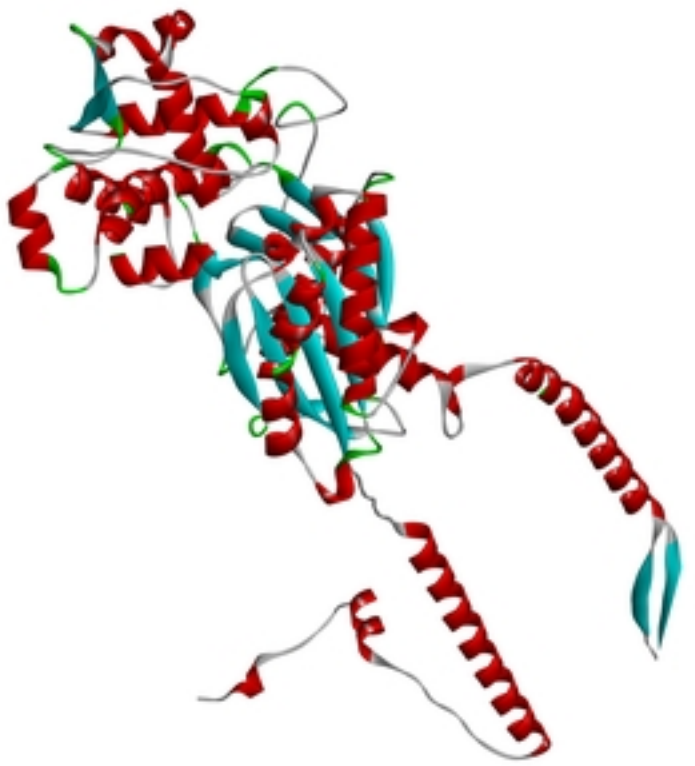

OsAPY5

OsAPY6

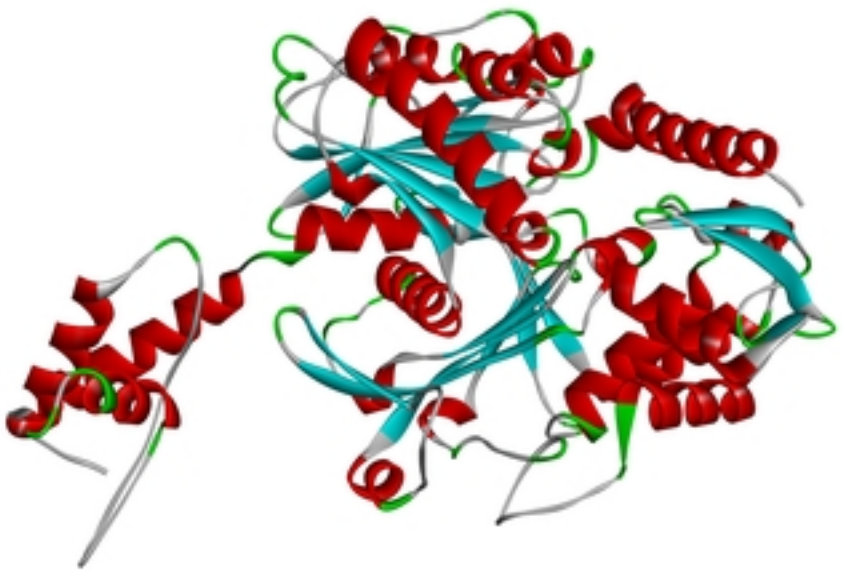

OsAPY7

OsAPY8

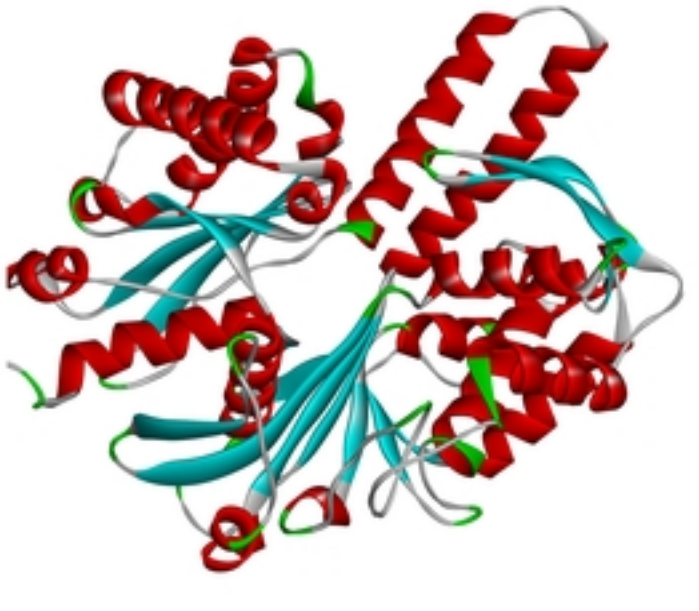

OsAPY9

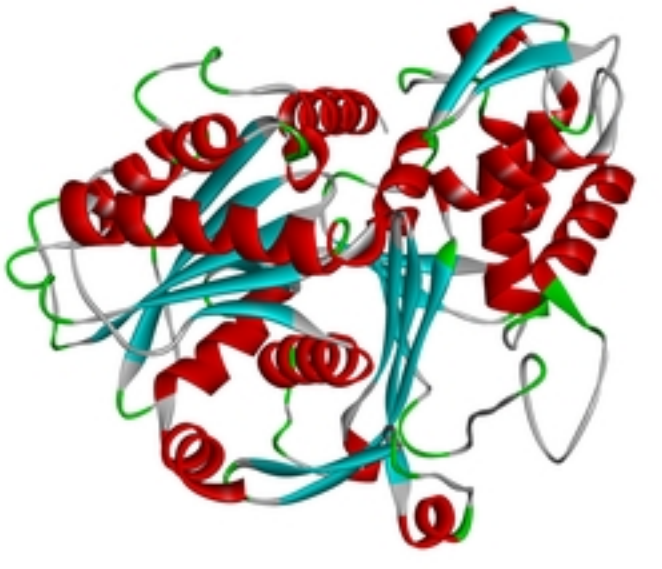

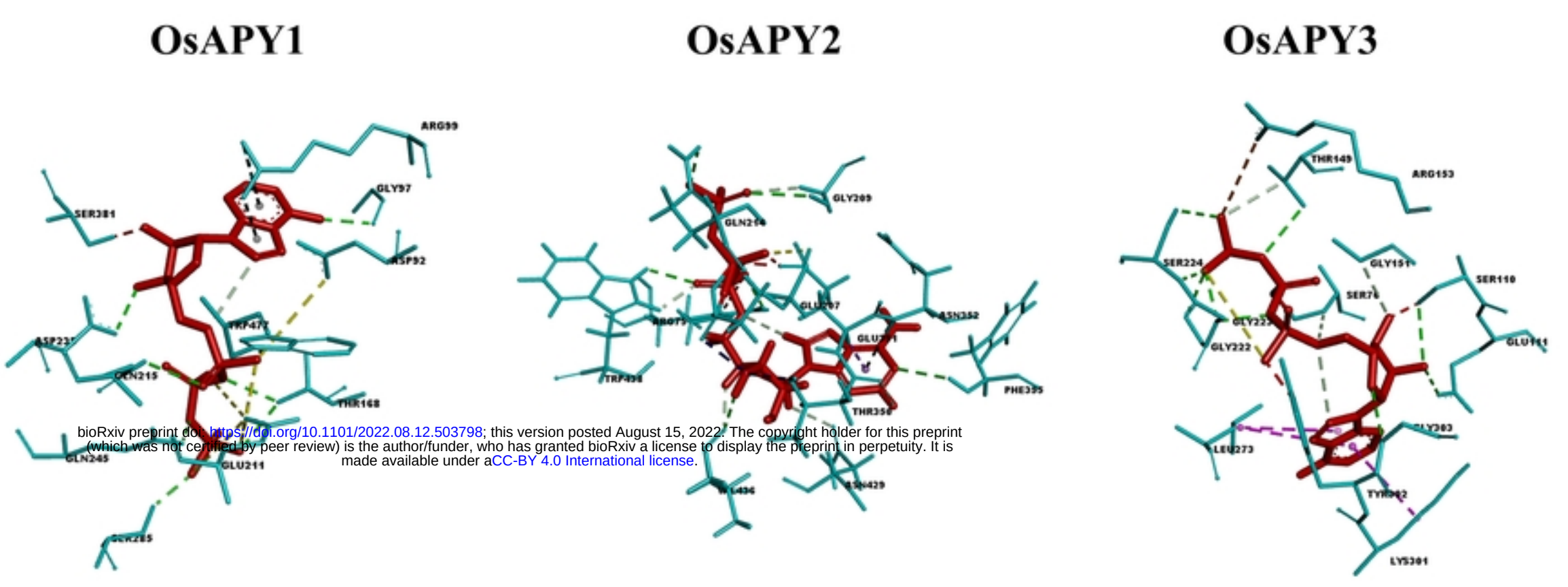

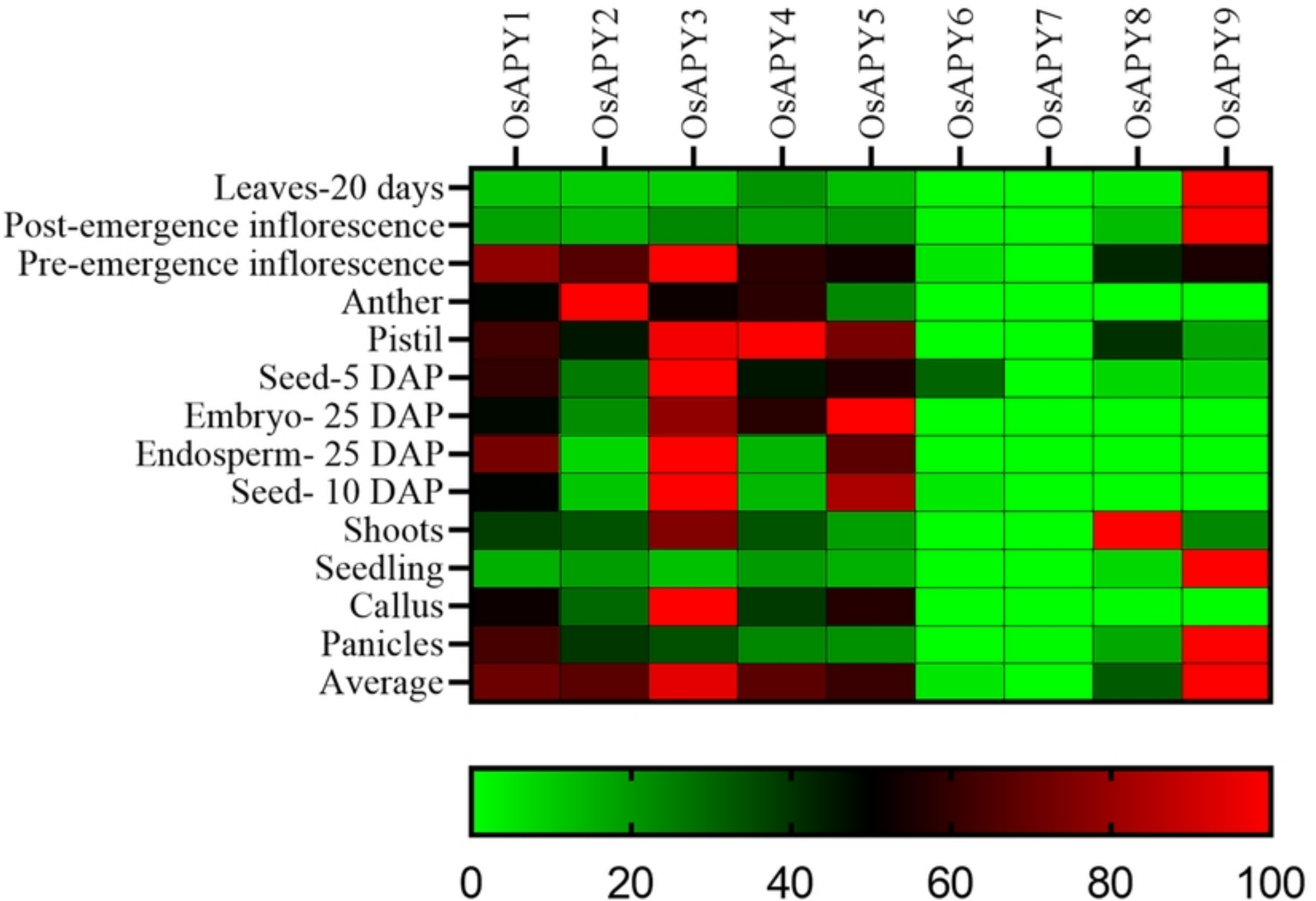
OsAPY1
OsAPY2
OsAPY3
OsAPY4
OsAPY5
OsAPY6
OsAPY7
OsAPY8
OsAPY9
Leaves-20 days
Post-emergence inflorescence
Pre-emergence inflorescence
Anther
Pistil
Seed-5 DAP
Embryo- 25 DAP
Endosperm- 25 DAP
Seed- 10 DAP
Shoots
Seedling
Callus
Panicles
Average
0
20
40
60
80
100

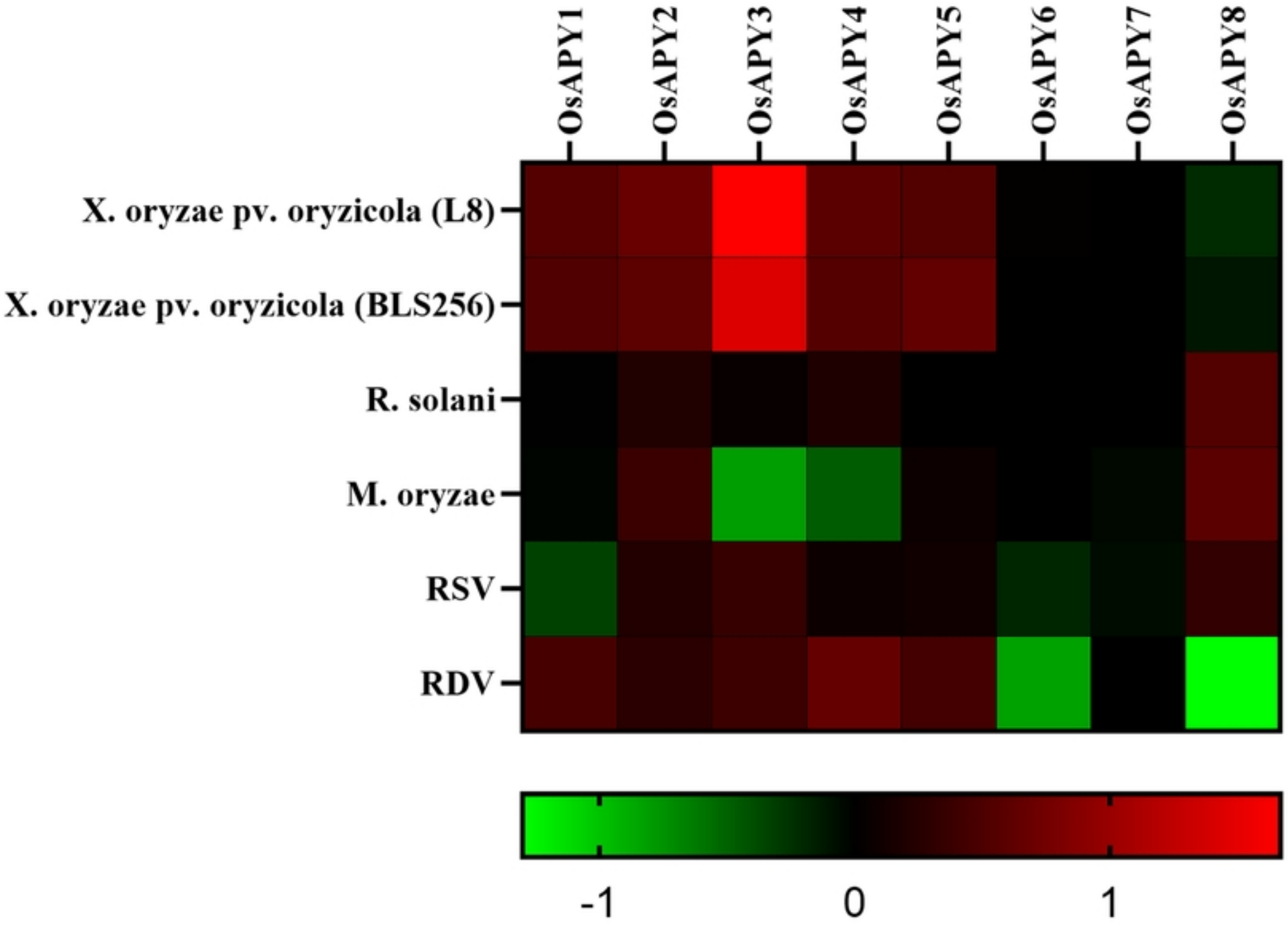
OsAPY1
OsAPY2
OsAPY3
OsAPY4
OsAPY5
OsAPY6
OsAPY7
OsAPY8
X. oryzae pv. oryzicola (L8)
X. oryzae pv. oryzicola (BLS256)
R. solani
M. oryzae
RSV
RDV
-1
0
1